bioRxiv preprint doi: https://doi.org/10.1101/2020.04.13.039503; this version posted April 15, 2020. The copyright holder for this preprint (which was not certified by peer review) is the author/funder, who has granted bioRxiv a license to display the preprint in perpetuity. It is made available under aCC-BY 4.0 International license.

Filovirus infection induces an anti-inflammatory state in Rousettus bats

Anitha D. Jayaprakash[a], Adam J. Ronk[b,c], Abhishek N. Prasad[b,c], Michael F. Covington[d], Kathryn R. Stein[h], Toni M. Schwarz[g], Saboor Hekmaty[h], Karla A. Fenton[c,e], Thomas W Geisbert[c,e], Christopher F. Basler[f], Alexander Bukreyev[b,c,e], Ravi Sachidanandam[h*]

a Girihlet Inc., Oakland, CA 94609

b Department of Pathology, the University Texas Medical Branch, Galveston, Texas, United States of America

c Galveston National Laboratory, the University of Texas Medical Branch, Galveston, Texas, United States of America

d Amaryllis Nucleics, Oakland, CA 94609

e Department Microbiology & Immunology, the University of Texas Medical Branch, Galveston, Texas, United States of America

f Center for Microbial Pathogenesis, Institute for Biomedical Sciences, Georgia State University, Atlanta, GA 30303, USA

g Department of Microbiology, Mount Sinai School of Medicine, New York, NY 10029

h Department of Oncological Sciences, Mount Sinai School of Medicine, New York, NY 10029

*Ravi Sachidanandam, E-mail: ravi.mssm@gmail.com

Abstract. The filoviruses Ebola (EBOV) and Marburg (MARV) cause severe disease in humans. In contrast, the Egyptian rousette bat (*Rousettus aegyptiacus*), a natural reservoir of MARV, exhibits a subclinical phenotype with limited MARV replication and nearly undetectable EBOV replication. Rousettus cell lines support replication of filoviruses, however. To understand the bat-filovirus interaction, transcriptomes of tissues from EBOV- and MARV-infected *R. aegyptiacus* bats were analyzed. While viral transcripts were only detected in liver, a systemic response was observed involving other tissues as well. By focusing on evolutionarily divergent (from human homologues) protein-coding genes, we identified novel transcriptional pathways that suggest infected bats exhibit impaired coagulation, vasodilation, aberrant iron regulation, and impaired complement system leading to muted antibody responses. Furthermore, a robust T-cell response and an anti-inflammatory state driven by M2 macrophages were identified. These processes likely control infection and limit pathology. All data can be freely explored and downloaded through our tools (http://katahdin.girihlet.com/shiny/bat/).

bioRxiv preprint doi: https://doi.org/10.1101/2020.04.13.039503; this version posted April 15, 2020. The copyright holder for this preprint (which was not certified by peer review) is the author/funder, who has granted bioRxiv a license to display the preprint in perpetuity. It is made available under aCC-BY 4.0 International license.

Introduction

Ebola virus (EBOV) and Marburg virus (MARV) are members of the family *Filoviridae*, which is comprised of filamentous, enveloped viruses with non-segmented, negative-sense RNA genomes[1]. EBOV and MARV cause outbreaks of severe, often fatal, disease in humans[2]. The second largest filovirus outbreak, caused by EBOV, is ongoing in the Democratic Republic of Congo and has resulted in 3,444 infections and 2,264 deaths as of March 2020[4]. The largest human outbreak of MARV occurred in Angola during 2004-2005, causing a reported 252 infections and 227 deaths[5]. Despite the aggressive use of a recently approved vaccine, control of the ongoing Congolese outbreak has been difficult, demonstrating the need for continued exploration of the pathobiology of these high-impact viruses.

There is substantial evidence that bats serve as hosts for filoviruses. MARV has been isolated from Egyptian rousette bats (*Rousettus aegyptiacus*) from sites in Uganda and Sierra Leone[6–8]. Ecological and experimental studies have demonstrated that these bats serve as a natural reservoir for MARV[7,9]. Circumstantial evidence suggests an association of bats with EBOV outbreaks[10,11]. Surveillance studies identified the presence of EBOV antibodies and RNA in several species of bats, implicating them as potential reservoirs of EBOV and other filoviruses[12]. However, infectious EBOV has never been isolated from a bat[12]. Additional evidence of association of filoviruses with bats has been obtained via detection of diverse filoviruses in bat tissues. These include Bombali virus (a novel species in the genus *Ebolavirus* identified in *Chaerephon pumilus* and *Mops condylurus* bats), Lloviu virus (the sole member of the genus *Cuevavirus* identified via RNA detected in *Miniopterus schreibersii* bats in Spain and Hungary), and Mengla virus (the sole member of the proposed genus *Dianlovirus* detected in the liver of a bat from the genus *Rousettus*)[13–17].

Experimental infections with MARV in Egyptian rousette bats have demonstrated virus replication in various tissues, but minimal clinical signs of disease. The virus is shed in saliva, urine, and feces[18–22]. Co-housed bats can transmit MARV from one individual to another[9]. A serial sacrifice study following subcutaneous inoculation of MARV demonstrated mild pathology as evidenced by transient elevations of alanine aminotransferase and, lymphocyte/monocyte counts as well as by modest levels of inflammatory infiltrates in livers[20,22]. Animals were able to clear MARV, and develop adaptive immune responses, including MARV-specific neutralizing IgG[23]. Serological data suggests the possibility that EBOV may infect bats of the *Rousettus* genus in nature[24–26] although it is unknown whether it was a systemic or abortive peripheral infection (often referred to as "exposure") with bats becoming seropositive as a result. EBOV can replicate in *R. aeqyptiacus* cell lines[27]. However, experimental inoculation of EBOV in these bats has not previously been associated with disease and has not produced definitive evidence of significant virus replication[27].

We experimentally infected Egyptian rousettes with EBOV and MARV and analyzed mRNA transcripts from multiple tissue types: liver, kidney, spleen, peripheral blood mononuclear cells (PBMCs), and testes. For that purpose, we compiled a comprehensive list of bat transcripts, based on our sequence data together with existing genome annotations[28], and, where possible, identified genes with human or mouse homologues.

The majority of the differentially-expressed genes upon filoviral infection were common to bats and humans[29]. These genes include components of a number of pathways involved in the innate, inflammatory, acute phase, and adaptive immune responses, as well as in the activation of the complement/coagulation pathway. Despite this broad similarity of the responses, filoviral infections *in vivo* result in very different outcomes in bats compared to humans.

bioRxiv preprint doi: https://doi.org/10.1101/2020.04.13.039503; this version posted April 15, 2020. The copyright holder for this preprint (which was not certified by peer review) is the author/funder, who has granted bioRxiv a license to display the preprint in perpetuity. It is made available under aCC-BY 4.0 International license.

Hypothesizing that this difference arises from altered function of evolutionarily divergent genes, we identified differentially expressed genes in *R. aegyptiacus* bats that also had significant differences in amino acid sequence relative to their human homologues. The pathways impacted by these genes suggest that they may be involved in the remarkable ability of bats to avoid clinical illness during filovirus replication. Our transcriptomics data suggest that unlike humans, infected bats 1) are in a state of impaired coagulation and increased vasodilation (which may have the effect of lowering blood pressure), 2) exhibit anti-inflammatory signatures including an early transition to an M2 macrophage phenotype and tissue regeneration in the liver, 3) exhibit downregulation of critical components of the complement system that facilitate antibody activity suggesting a muted antibody response (to MARV[7]), and 4) appear to mount a robust T cell response, which is a component of successful viral clearance in humans.

This is the first comprehensive *in vivo* study of the transcriptomic changes induced by filovirus infection in bats. Our results highlight key parts of the systemic response that facilitate the ability of bats to survive filovirus infections and suggest potential host-targeted therapeutic strategies with utility in human infection.

MATERIALS AND METHODS

Experimental methods

Viruses. Recombinant wild-type EBOV, strain Mayinga, was recovered from the full-length clone and support plasmids in HEK 293T cells and passaged twice in Vero E6 cells for amplification, as described previously[29]. Recombinant wild-type MARV, strain Uganda, was recovered similarly in BHK-21 cells as described previously[30] and was also passaged twice in Vero E6 cells for amplification.

Bat experimental protocol. Adult Egyptian rousettes were obtained from a commercial source and quarantined for 30 days under ABSL-2 conditions. Animals were implanted with microchip transponders for animal ID and temperature data collection. For studies with EBOV and MARV, animals were transferred to the Galveston National Laboratory ABSL-4 facility. Animals were segregated into groups of three. Except for one MARV-infected male, all bats were female. Each group was housed in a separate cage for inoculation with the same virus. After acclimation to the facility, animals were anesthetized with isoflurane and infected subcutaneously in the scapular region with 10^5 focus forming units (FFU; titrated on Vero E6 cells) of EBOV or MARV. Every other day, animals were anesthetized by isoflurane, weighed, temperature was determined via transponder, and 100-150 µL of blood was collected from the propatagial vein. Nucleases in blood were inactivated in 1 mL of TRIzol reagent (Thermo-Fisher Scientific). Samples were then removed from ABSL-4 containment, and RNA was extracted. Droplet-digital RT-PCR (ddRT-PCR) with primers specific to the nucleoprotein (NP) gene was used to detect viremia. If fewer than 10^6 MARV RNA copies/mL viremia were detected in a MARV-inoculated bat, the animal was observed for additional 2 days to allow the animal to reach a higher viral RNA load. In 48-96 hours after first observation of viremia, the animal was euthanized under deep isoflurane sedation via cardiac exsanguination confirmed by bilateral open chest. All EBOV-inoculated bats were euthanized 48 hours after the first detection of viremia, independent of viral RNA load. Tissues were collected (listed in **Table S1**) and immediately homogenized in an appropriate volume of TRIzol reagent and stored at -80°C. Tissue sections were also homogenized in minimal essential media (MEM) supplemented with 10% fetal bovine serum and stored at -80°C. Additional tissue sections were fixed in 10% neutral buffered formalin for histopathology.

bioRxiv preprint doi: https://doi.org/10.1101/2020.04.13.039503; this version posted April 15, 2020. The copyright holder for this preprint (which was not certified by peer review) is the author/funder, who has granted bioRxiv a license to display the preprint in perpetuity. It is made available under aCC-BY 4.0 International license.

Tissues and PBMCs were also collected from three uninfected control animals. Given that the course of infection appears to be relatively short in these animals[21], we sacrificed them shortly after onset of viremia in the infected animals to ensure adequate capture of changes in transcriptional dynamics. As such, animals were bled every other day, and viral loads were assessed via ddRT-PCR. In addition, animals were weighed, and temperature was determined with each bleed.

All animal procedures were performed in compliance with protocols approved by the Institutional Animal Care and Use Committee at the University of Texas Medical Branch at Galveston.

Leukocyte isolation. Leukocyte isolation was performed using ACK lysis buffer (Gibco). Ten volumes of lysis buffer were added to whole blood, incubated for 2-3 minutes, and then neutralized with complete DMEM media containing 10% FBS. Following neutralization, samples were centrifuged at 250 *g* for 5 minutes at 4°C, after which the supernatant was decanted from the pellet. This process was repeated several times per sample until a white pellet of cells free of contaminating red blood cells remained. Density gradient purification was not performed on these samples prior to or after red blood cell lysis; therefore, these leukocyte populations were assumed to contain granulocytes in addition to PBMCs.

mRNA sequencing. Total RNA was isolated from bat tissues using Ambion's RNA isolation and purification kit. For most samples, polyA-tailed mRNA was selected using beads with oligo-deoxythymidine and then fragmented. A few samples with poor (RNA Integrity Number) scores were treated with Ribominus (targeting human ribosomal RNA) to enrich for polyA-tailed mRNA before fragmentation. cDNA was synthesized using random hexamers and ligated with bar-coded adaptors compatible with Illumina's NextSeq 500 sequencer. A total of 88 samples were sequenced on the NextSeq 500, as 75 base pair single reads.

Analytical methods

Transcripts. We built a custom non-redundant reference bat mRNA sequence database, which is available on the shiny website. The issue of splice variants was avoided by keeping only the longest transcript for each gene. We used transcripts from different bat species and added missing annotations/sequences (e.g., CYP11B2 and PLG) to our database by assembling reads from our own sequence data. These required custom scripts as the support for transcripts was not always robust enough to use standard tools, due to low coverage and/or gaps in the transcripts. The gene sequences are collected from different bat species, so error-free reads might not map perfectly to the transcripts in the database. The database has sequences of 18,443 bat mRNAs, and include EBOV and MARV sequences, the infectious agents used in our studies. The genes were identified by homology to mouse and human genes. Most genes (16,004) had high similarity to human or mouse homologues, as defined by BLASTn with default settings identifying matches spanning the length of the mRNA.

We label the set of remaining genes (2439) as divergent and use these transcripts to identify systemic differences between the bat and human responses to filovirus infections. Of these, a smaller set (1,548 transcripts) could be identified by increasing the sensitivity of BLASTn by reducing the word-size from 11 to 9, which is equivalent to matching at the protein level. The remaining 891 putative transcripts could not be reliably identified by homology. Of these 891 transcripts, homologues for 182 could be identified on the basis of partial homology and domain structure, while the remainder (709 sequences whose names start with UNDEF) belonged to one of four classes, 1) aligned to un-annotated transcripts in the human genome, 2) non-coding RNAs, 3) transcripts unique to bats, or 4) assembly errors. We use capitalizations to represent bat gene symbols, as in the human gene nomenclature.

bioRxiv preprint doi: https://doi.org/10.1101/2020.04.13.039503; this version posted April 15, 2020. The copyright holder for this preprint (which was not certified by peer review) is the author/funder, who has granted bioRxiv a license to display the preprint in perpetuity. It is made available under aCC-BY 4.0 International license.

Expression Analyses. Kallisto was used to determine transcript expression levels from reads. Kallisto uses pseudo-alignments and is relatively more accepting of errors/variants in reads[31]. This is the appropriate tool to quantify transcripts in the samples, as the mRNA sequences from different species can have mismatches to error-free reads. Kallisto uses a parameter "k" while indexing the database to specify how sensitive it is to matches with smaller k values leading to more spurious hits. We empirically determined k=23 to be an appropriate parameter value with which to index the reference mRNA dataset. We used the transcripts-per-million (tpm) value as the transcript expression levels to determine changes in expression across samples.

We used the presence of viral transcripts to confirm proper assignment of samples. This approach has previously helped us to identify and correct mistakes of annotation in some of the cell line data and also identified a problem with a published dataset[32], where all the naïve (uninfected) samples showed signs of viral infection. Furthermore, to ensure there was no mislabeling of samples from individual bats, we identified single nucleotide variants to ensure that all tissue samples from an individual had the same set of variants

Tools for data exploration and interrogation. We developed a web browser-based tool using *Shiny* in R, which is accessible at http://katahdin.girihlet.com/shiny/bat/. This allows exploration of the data across various samples on a gene-by-gene basis, as well as analysis of viral expression in the samples. Samples can also be compared using scatter plots and hierarchical clustering. Data from the outlier excluded from our analyses is available in the online tool.

Statistics. Datasets obtained from in vivo studies are inherently noisy, for a variety of biological reasons: viral replication and infection of cells is variable across samples/tissues and the samples consist of a heterogenous mixture of cell types that can vary from sample to sample, even from the same tissue type. Bats can also be infected by other pathogens in addition to the filovirus. Large changes in expression profiles were readily detected by comparing averages across replicates, since such changes are less affected by noise; however, subtle changes (less than 2-fold) were difficult to reliably detect due to lack of power in the sample size and variability between samples. To accommodate this most effects noted in our study are greater than 2-fold up- or down-regulated.

Pathway analyses. A basic assumption underlying our study is that bats are mammals that possess innate and adaptive responses to infections that roughly mirror those seen in humans. The data from comparative filovirus infections in human and bat cell lines supports this.[29] Despite similarities in the basic architecture of the networks, effects seen at the organismal level are likely to arise from subtle differences in the systemic responses. We were, therefore, able to guide our analysis by what is known from human and mouse studies of the relevant pathways and genetic networks.

We identified pathways of interest, based on divergent genes that were differentially expressed in bat liver upon filovirus infection, as explained in the results (**Fig. 3**).

RESULTS

Clinical, virological, and pathological findings in inoculated bats

Inoculated bats showed no apparent clinical signs or changes in behavior, and body weights and temperatures remained relatively constant (**Fig. 1-I,II**). Viral RNA was detected (using ddRT-PCR) in the blood of MARV-inoculated animals earlier (and higher) than in the EBOV-inoculated animals (**Fig. 1-III**), particularly in the liver, spleen, and kidney samples. We examined the potential for excretion via salivary glands and urine in

bioRxiv preprint doi: https://doi.org/10.1101/2020.04.13.039503; this version posted April 15, 2020. The copyright holder for this preprint (which was not certified by peer review) is the author/funder, who has granted bioRxiv a license to display the preprint in perpetuity. It is made available under aCC-BY 4.0 International license.

MARV-inoculated bats. Two of three animals had virus detectable by plaque assay in the salivary glands, while one of three animals had detectable virus in the kidneys (**Fig 1-IV**). The virus was not detected by plaque assay (limit of detection is 10 Pfu/cc) in most or all tissues collected from EBOV-inoculated animals (**Fig 1-V**).

In MARV-infected animals, histopathological observations were largely consistent with prior publications[18,21]. For MARV-infected animals, cytoplasmic immunostaining was performed using a pan-filovirus antibody. In these bats, we observed diffuse cytoplasmic immunostaining with moderate frequency in the absence of histopathological lesions in the mammary glands and testes, suggesting presence of virus in these organs. Two of the three EBOV-inoculated animals presented with noteworthy histopathological lesions in the liver, consisting of pigmented and unpigmented infiltrates of aggregated mononuclear cells compressing adjacent tissue structures, and eosinophilic nuclear and cytoplasmic inclusions. Focal EBOV immunostaining was observed in the liver of one animal, using both pan-filovirus and EBOV-VP40 antibodies, but very few foci were found, suggesting low viral replication (**Fig 1-VI**). Since the animals did not come from a colony known to be pathogen-free and viral loads were determined to be extremely low, any connections between the histopathology and EBOV infection are unclear.

Filovirus infection of bats results in a significant and consistent response in the transcriptome

mRNA from tissues (liver, spleen, kidney, lungs, salivary glands, large and small intestine, and testes) collected from infected and uninfected bats was deep sequenced. Multi-dimensional scaling (MDS, **Fig. 2A**) established that one non-infected control bat liver sample (labeled ***cb1*** in the shiny tool) seemed to be an outlier compared to the other two (***cb2*** and ***cb3*** in the shiny tool); many inflammatory genes were upregulated in this sample , suggesting that ***cb1*** may have had an unexpected injury or infection. Although we left ***cb1*** out of the analysis, ***cb1*** data are available for exploration in the shiny tools.

Consistent with the fact that liver is one of the main targets of MARV[33] and abundant viral transcripts were present only in the liver samples, we expected to detect robust transcriptional response in the liver tissue. However, samples from other tissues also clustered separately based on the type of infection (MARV, EBOV and mock, **Fig. 2B, S1**). This suggests that even though the liver was the focus of replication, the response to infection was system wide.

We summarize the effect of filoviral infection on the liver transcriptome using an upset plot (**Fig. 3),** which is just another way of drawing a Venn diagram, showing membership of genes in six sets (genes up/down regulated in EBOV-infected samples compared to mock-infected samples, genes up/down regulated in MARV-infected samples compared to mock-infected samples, and genes up/down regulated in EBOV-infected samples compared to MARV-infected samples). The various intersections between the sets show members unique to that intersection. A large set of genes was found to respond to infection with either virus, indicating the response is broader than a simple perturbation of the naïve state. We also found that more genes responded to MARV infection than to EBOV infection, concordant with more robust replication of MARV in these animals (**Fig. 3**).

As such, most of our analyses concentrated on liver RNA transcripts. For some genes, we also analyzed transcriptional response in kidneys and/or spleens in order to understand the regulation of certain pathways (e.g., Renin is expressed in kidney and regulates the blood pressure system).

Responsive, evolutionarily divergent bat genes guide pathway analysis

bioRxiv preprint doi: https://doi.org/10.1101/2020.04.13.039503; this version posted April 15, 2020. The copyright holder for this preprint (which was not certified by peer review) is the author/funder, who has granted bioRxiv a license to display the preprint in perpetuity. It is made available under aCC-BY 4.0 International license.

Genomic and transcriptomic datasets provide a rich field for developing theories, but they can also be minefields when the analysis is carried out without guidance from the relevant biology. Routine pathway analyses using standard tools usually result in lists of pathways/functions replacing gene lists, often without offering much additional insight. If we start with the full list of genes responsive to filovirus infections, the list will be dominated by the interferon response genes, obscuring the pathways responsible for the systemic response. The multiple testing problem becomes apparent at this level because, with the large set of responsive genes it is not clear which genes are important and if some are highlighted due to random chance

To guide our exploration of the datasets, we identified a set of bat genes (2439 genes) with significant differences from their human/mouse homologues, defined as genes whose homologues could not be identified using BLASTn with default settings. This is based on our hypothesis that these divergent genes must be the foundation of the differences in the systemic responses to filoviruses between bats and humans systemic. Considering only genes with reasonable expression (tpm > 20) in at least one class of liver samples (MARV-, EBOV- or mock-infected) we refined the list down to 264 genes. Of these, 151 genes were responsive in at least one class of bat livers, defined as up- or down- regulated at least 2-fold upon infection with EBOV or MARV. This process of narrowing down the list of genes of interest is depicted in **Fig. 4**.

Tables S1-S8 show the 151 genes split into various classes, upregulated (the log2 ratio to the mock-infected sample is greater than 0.6) in both, downregulated (log2 ratio to the mock-infected samples is less than -0.6) and various combinations thereof. The tables have annotated various pathways/processes that the genes participate in. The major themes identified by this preliminary analysis and the connections between them are outlined in **Fig. 5**. We found that the following pathways/systems were impacted by filovirus infection: acute phase proteins (**Table 1**), interferon responsive genes (**Fig. 6,7**), macrophage polarization (**Fig. 8,9,10**), the complement system (**Fig. 11**), the adaptive immune system (**Fig. 12**) and the vascular system (**Fig. 13,14,15**).

Infected bats have transcriptional profiles indicative of a robust innate immune response to filovirus infection

We detected a robust innate immune response *in vivo* not only to MARV, but also to EBOV, despite limited viral replication. Innate immune genes are seen to be responsive to MARV and EBOV infection (**Fig. 5,6,7**). Our previous *in vitro* transcriptomic studies demonstrated that the innate immune response in bat cells is broadly similar to that in human cells[29]. Additionally, most innate immune bat genes are not divergent from their human homologs, as we have defined it. Thus, we believe that the innate immune response likely cannot explain, on its own, the drastic difference in infection phenotype observed in bats relative to humans.

Infected bats exhibit an acute phase response, involving multiple acute phase proteins (APP)

Inflammation and injury[34,35] trigger inflammatory cytokines (e.g., Interleukin-1(IL-1), IL-6, and TNFα). These cytokines subsequently trigger transcriptional events that lead to an increase in serum levels of some acute phase protein (APP)[36] and a decrease of others (e.g., transferrin, albumin[37]). APPs are produced by hepatocytes in the liver, and are an important part of the innate immune response.[38] Depending upon the combination of cytokines, the specific reaction can vary in response to different inflammatory conditions.[39–41] The IL-6 response is often not directly detected by mRNA-seq data due to low expression; however, the APPs respond strongly.

Our data indicates that MARV infection, and to a lesser extent EBOV infection, elicits a strong APP response in bats (**Table 1**). SAA expression, for example, increased 1,000-fold in response to MARV infection. Curiously,

bioRxiv preprint doi: https://doi.org/10.1101/2020.04.13.039503; this version posted April 15, 2020. The copyright holder for this preprint (which was not certified by peer review) is the author/funder, who has granted bioRxiv a license to display the preprint in perpetuity. It is made available under aCC-BY 4.0 International license.

c-reactive protein (CRP), known as a marker for inflammation/acute-phase-response in humans, was not expressed in bat livers. Potentially, CRP may not be present in an active form in bats at all (**Table 1**).

Persistent expression of IL-6, known to cause chronic inflammation, is tightly regulated via negative feedback loops. We found that several of these negative feedback loops were strongly upregulated in liver tissues in response to MARV infection and to a lesser degree in response to EBOV infection. These include 1) GP130 (IL-6ST), which acts to initiate the Janus kinase (JAK)-STAT3 pathway, 2) STAT3, which induces various IL-6 responsive genes such as APPs and the SOCS (suppressor of cytokine signaling) genes, and 3) the SOCS genes themselves, which bind to JAK and GP130 to stop IL-6 signaling (**Fig. 6,7**).

Inflammation is also mediated by leukotrienes (LTC4) and prostaglandin E, which are produced by microsomal glutathione S-transferases (MGST1 and MGST2)[42]. Under filoviral infection in bats, MGST1 and MGST2 are highly upregulated.

Infected bats exhibit a transcriptional profile suggestive of an early transition from an M1 dominated to an M2 dominated macrophage population

Macrophages recognize and phagocytize foreign organisms and damaged host cells. Macrophages, an important early target for filoviruses[43], play a major role in the immune response in the liver, one of the primary sites of filovirus replication. Macrophages can be either in an M1 state (inflammatory, assisting innate immunity) or in an M2 state (anti-inflammatory, assisting tissue regeneration) (**Fig. 8,9,10**) and can polarize or shift from one state to the other. Key markers of M1 macrophage activation include IRF5, NF-κB, AP-1, and STAT1 (**Fig. 8**), which subsequently lead to the secretion of pro-inflammatory cytokines such as IFN-γ, IL-1, IL-6, IL-12, IL-23 and TNFα.

M2 macrophages have additional anti-inflammatory subclasses (M2a, M2b and M2c) that share some markers and are distinguished by others[44]. M2a macrophages enhance tissue regeneration and inhibit inflammatory responses. They are activated by IL-4 and IL-13, which, in turn, upregulate arginase-1(ARG1), IL-10 and TGF-β[45]. The M2b macrophages have anti-inflammatory activity by producing IL-1, IL-6, IL-10, TNF-α. M2c macrophages suppress inflammatory response. They are activated by IL-10, transforming growth factor beta (TGF-β), and glucocorticoids, and they produce IL-10 and TGF-β. In the anti-inflammatory state, mitochondrial activity is increased and primarily involved in fatty acid metabolism.

Prolonged M1 activity can be harmful and is modulated by the negative feedback that transforms macrophages from M1 to M2 state[46,47], thereby controlling inflammation during infections and the transition to tissue repair [48,49] (**Fig. 8**). M1 macrophages rely upon glycolysis and M2 macrophages utilize fatty acid oxidation as an energy source. The switch between states is achieved by simply disrupting cellular energy metabolism. M2 macrophage polarization is accompanied by mitochondrial biogenesis. Hypoxia-inducible factor 1 (HIF1) is a key regulator inducing M2 polarization through hypoxia[50]. HIF1A[51–53], promotes mitophagy and is required by M1 macrophages, whereas M2 macrophages depend on the mitochondrial oxidative metabolism. Inactivating HIF1A also promotes M2 polarization.

We found that filovirus-infected bats exhibit upregulation of key markers of M1 macrophages, including IRF5, NF-κB, AP1G1 (a subunit of the AP-1 complex), and STAT1 (**Fig. 6,7**). These lead to the secretion of pro-inflammatory cytokines such as IFN-γ, IL-1, IL-6, IL-12, IL-23 and TNFα, all of which were upregulated in filovirus-infected bats, which we infer through either direct or indirect evidence. Expression of these markers

bioRxiv preprint doi: https://doi.org/10.1101/2020.04.13.039503; this version posted April 15, 2020. The copyright holder for this preprint (which was not certified by peer review) is the author/funder, who has granted bioRxiv a license to display the preprint in perpetuity. It is made available under aCC-BY 4.0 International license.

was stronger in MARV-infected animals, corresponding to greater replication of the virus, but it is difficult to clearly delineate the cause/effect relationship.

Although we did not detect expression of IL-4 and IL-13 in any bat tissues, genes regulated by them, such as MRC1, TGFB1 and ARG1 were found to be highly expressed in livers of bats infected with both viruses. CSF1 is a cytokine that controls the production, differentiation, and function of macrophages. The CSF1 receptor (CSF1R) that mediates the biological functions of CSF1 was also upregulated in filovirus infected bat livers, the upregulation was greater in EBOV infected animals (**Fig. 8,9**). Several genes related to fatty acid oxidation were found to be upregulated by filovirus infection (**Tables 1-3**). Infected bats also upregulated multiple markers of mitochondrial abundance, such as TFAM, OPA1, MFN1/2, and DNM1L, more so in MARV than in EBOV. The pyruvate dehydrogenase, PDK1, involved in the response to hypoxia was also upregulated (more so in MARV than EBOV) [54]. HGF-MET and PPARGC1A involved in mitochondrial biogenesis[55], are upregulated upon MARV infection.

In MARV-infected bats, SOCS3, which promotes M1 polarization, was upregulated. Several M2 markers, including TGFB1, ARG1, and MRC1 were also upregulated (**Fig. 8,9**). Additional evidence for M2 polarization is provided by the non-anemic state of EBOV-infected bats, inferred from the presence of abundant iron, which enhances macrophage M1 to M2 polarization.[56]

PKM, HIF1AN and HGF, which play an important role in inactivating HIF1A to promote the M1 to M2 switch, are all upregulated in filovirus infected bats (**Fig. 8,9**).

Finally, the gene GPD2, the mitochondrial glycerol-3-phosphate dehydrogenase which contributes to the shift in core metabolism in macrophages associated with the M1 to M2 transition during infection aiding tissue repair[57] was found to be upregulated by filovirus infection (**Fig. 9**).

These findings indicate that bats may transition from an M1-dominated macrophage response to an M2-dominated response relatively early in infection compared to humans. This switch may be an important component of the ability of the animals to control infection and avoid clinical disease by suppressing inflammation and promoting tissue regeneration. This would reduce or prevent immunopathology and allow the adaptive immune system to effectively control the virus.

Expression of key components of the classical complement pathway is inhibited by filoviral infection

The complement pathway has three branches, the classical pathway, the mannose-binding lectin pathway and the alternative pathway[58]. The classical pathway recognizes antigens bound to antibodies; the lectin pathway binds to sugar molecules on the virus particles and the alternative pathway is a component of the innate defense against infections.

Both the classical and lectin complement pathways were activated by filovirus infection (**Fig. 11**). However, several elements of the classical pathway were downregulated or even not expressed in filovirus infected livers, including C1R, C3, C8G, and MASP2. Downregulation or suppression of expression of C1R, C3, and MASP2 would compromise the classical pathway as they are key to the antibody effector activity. This likely reduces the efficiency of the antibody activity in infected bats, consistent with the finding that antibody-mediated virus neutralization is not the dominant mode for filovirus clearance in *R. aegyptiacus* bats.[59]

Infected bats exhibit transcriptional signatures of robust T cell activity

bioRxiv preprint doi: https://doi.org/10.1101/2020.04.13.039503; this version posted April 15, 2020. The copyright holder for this preprint (which was not certified by peer review) is the author/funder, who has granted bioRxiv a license to display the preprint in perpetuity. It is made available under aCC-BY 4.0 International license.

We found that multiple markers of CD8+ T cell activity, including CCL3, ANAX1, TIMD4 and MAGT1 were upregulated by filovirus infection (**Fig. 12**), indicating that bats may mount a strong cellular response despite the apparent weakening of the humoral response. Overall, this suggests that control and clearance of filovirus infection in bats may largely depend upon a robust cellular response, similar to what has been observed in humans, where individuals who recover tend to mount robust cellular responses.[60–62]

Infected bats exhibit dramatic signatures in the vascular system, with low coagulation, vasodilation and non-anemic states despite HAMP upregulation

Three major interconnected pathways of the vascular system are, a) iron metabolism (**Fig. 13**), b) blood pressure (**Fig. 14**) and c) coagulation (**Fig. 15**). The interplay between the three is complicated (outlined in **Fig. 5**). We highlight genes involved in the response affecting the three pathways and the connections between them. To better present our results in context, give a brief overview of iron metabolism.

Iron, an essential component of heme needed for oxygen transport, is tightly regulated, [63] mostly by hepcidin (HAMP)[64](**Fig. 13**). HAMP controls the internal absorption of iron[65], by binding Ferroportin (SLC40A1/FPN1), to block export of iron across membranes and cause Ferroportin degradation. HAMP is upregulated by iron in serum and pro-inflammatory stimuli (IL-6), such as infection.[66] In blood, iron forms a complex with Transferrin (TF), which is enabled by ceruloplasmin (CP) and MOXD1, involved in processing copper.[67]

In the cytosol, iron is bound to ferritin (comprised of a heavy chain, FTH1 and a light chain FTL), synthesized by cells in response to increased iron. Thus, ferritin is a marker for iron levels in serum.[68] In mitochondria, iron is bound to FTMT**,** the mitochondrial ferritin.[69] PCBP2, an iron chaperone is also needed for iron transport within the cytosol[70]. STEAP3 helps transport iron from Transferrin to the cytosol of erythrocytes[71].

Most iron is in hemoglobin (66%), the remainder is stored mostly in macrophages in the liver, which take up iron through the CD163 receptor. The bone marrow can suppress HAMP synthesis, in response to anemia, leading to export of iron from macrophages, and increased uptake of iron from diet.

In EBOV- and MARV-infected bat tissues, HAMP was upregulated (**Fig. 13**). In MARV infection, macrophage expansion/infiltration (as was observed in histology sections of infected tissues) and lowered hemoglobin expression suggest that red blood cell production might be impaired, which is potentially a sign of anemia. Further, CD164, which suppresses hematopoietic cell proliferation, was also upregulated by MARV infection (**Fig. 13**).

In EBOV-infected bats, FTH1 and FTMT were both upregulated (**Fig. 13**), reflecting increased iron abundance in serum. In contrast, FTH1 and FTMT, along with PCBP2 were downregulated in MARV-infected bats. Upregulation of HBB in EBOV-infected samples was also observed. This suggests that hematopoiesis was impaired in MARV-infected bats, but not in EBOV-infected bats. It is likely that this was a result of the divergent pathobiology of EBOV and MARV infections in Egyptian rousettes. The early control of EBOV by these bats suggest that the iron levels in bats that eventually clear MARV infections may resemble the iron levels in EBOV-infected animals.

Filovirus-infected bats exhibited transcriptional signatures of vasodilation, which may indicate a low blood pressure state

Blood pressure (**Fig. 14**) can be controlled by either vasoconstriction (e.g., AGT2 activity and the renin/angiotensin system), or by changing the concentration of salts in blood (e.g., regulation of aldosterone by

bioRxiv preprint doi: https://doi.org/10.1101/2020.04.13.039503; this version posted April 15, 2020. The copyright holder for this preprint (which was not certified by peer review) is the author/funder, who has granted bioRxiv a license to display the preprint in perpetuity. It is made available under aCC-BY 4.0 International license.

CYP11B2). The primary means of blood pressure regulation is renal expression of renin, which converts Angiotensinogen to Angiotensin I. Angiotensin converting enzyme (ACE) converts Angiotensin I to Angiotensin II, which constricts blood vessels to increase pressure. ACE expression is upregulated by a feedback loop triggered by low blood pressure. Angiotensin II also enhances production of active plasmin increasing coagulation, connecting the pressure and coagulation pathways[72]. Inflammation upregulates the SERPIN genes, several complement genes, and HAMP, which connects the iron, blood pressure and coagulation pathways. Prostaglandin I2 synthase (PTGIS), which inhibits platelet aggregation and reduces blood pressure, CYP11B1 and CYP11B2 (which reduce blood pressure and inflammation) all connect blood pressure, inflammation and coagulation[73].

During filovirus infection in bats, we found that ACE was upregulated, while angiotensin and AGT were downregulated (**Fig. 14**). Additionally, we found that PTGIS was upregulated. In EBOV-infected bats, CYP11B2 (which regulates blood pressure by synthesizing aldosterone) was upregulated (**Fig. 14**)

The vascular response might be another key to the response of bats to filovirus infection. Humans infected with EBOV or MARV in many cases eventually exhibit excessive bleeding, low blood pressure, and excessive and dysregulated coagulation in the form of disseminated intravascular coagulation[74]. Our data suggest that bats use multiple strategies to protect their vascular systems during filovirus infection, an important mechanism for limiting the pathology.

DISCUSSION

The ability of bats to serve as hosts for a variety of diverse viruses has been a topic of considerable interest and scientific attention, with several theories being proposed to explain this phenomenon.

One theory posits that bats have constitutively expressed interferons or permanently active innate immune system, ready and waiting for pathogens to appear[75], although this has not been a universal observation in all bat species[76,77]. The reported levels of constitutive expression reported[75] are extremely low (at least 5 orders of magnitude lower than ribosomal RNA), which makes them undetectable in mRNAseq, but also raises questions about nature of the constitutive expression. Further, in an mRNA-seq study on PBMCs from EBOV-infected humans, individuals who succumbed to disease showed stronger upregulation of interferon signaling and acute phase response-related genes compared to survivors during the acute phase of infection[82]. Therefore, the differences in responses between human and bats goes beyond any upregulation or constitutive expression of interferons.

Another theory suggested that components of the innate immune response (e.g., STING(TMEM173)) could be mutated to become less effective in bats[78]. It is unlikely that a single gene is the “magic bullet” that explains the profound differences observed between human and bat responses to filovirus infection. Instead, our data together with the extant literature strongly suggest that modifications of entire systems is required to produce the observed divergence in the response to infection.

The innate response of human and bat cell lines to filovirus infections is almost identical, but *in vivo*, the clinical course and outcomes in humans and bats are different. Such differential responses likely involve a variety of tissue/cell types and the interactions between them are driven by numerous genes. Identifying divergent genes in this large set and using them to identify the systemic differences between bats and humans provides a rational basis for the analysis of this data. By limiting ourselves to genes that fit this requirement, the multiple testing problem was ameliorated, by drastically reducing the number of genes being considered.

bioRxiv preprint doi: https://doi.org/10.1101/2020.04.13.039503; this version posted April 15, 2020. The copyright holder for this preprint (which was not certified by peer review) is the author/funder, who has granted bioRxiv a license to display the preprint in perpetuity. It is made available under aCC-BY 4.0 International license.

A study in humans infected with EBOV[83] analyzed 55 biomarkers in blood, showing viremia to be associated with elevated levels of tissue factor and tissue plasminogen activator, which is consistent with coagulopathy. Nonfatal cases had higher levels of sCD40L expression, a marker for T cell activity, consistent with our data that suggest that T cells are highly active during filovirus infection of bats while antibody-mediated virus neutralization is potentially less important for filovirus clearance[59].

The state of the bat under filoviral infection and the fact that they do survive these infections suggests potential approaches to helping human patients.

We believe the anti-inflammatory state induced in bats upon filovirus infection is a natural application of this strategy, especially the early switch to M2 macrophage polarization. This allows the adaptive defenses of bats to clear the virus and avoid damage from immunopathology.

Thus, an attempt could be made to reduce the human hyperinflammatory response[88] to filovirus infections by modulating the innate response to prevent damage and allow other processes to clear the infection and allow for wound healing. For example, Anti-inflammatory agents could also be used to emulate the protective physiological conditions observed in bats (e.g., through the inhibition of IL-6). One approach would be to target the IL-6 receptor through the use of tocilizumab (Actemra), an antibody directed against the IL-6-receptor[95]. Alternatively, IL-6 could be targeted directly with agents such as siltuximab (Sylvant)[96]. Another class of anti-inflammatory agents are LTC4 inhibitors, used to treat asthma, may be of benefit in filovirus infection which in bats upregulate MGST1 and MGST2, in turn inducing leukotrienes (LTC4) and prostaglandin E, which are mediators of inflammation[42].

Our evidence further suggests that bats, upon infection by filovirus, may naturally vasodilate and reduce their blood pressure (mimicking the action of ACE inhibitors). They further make the endothelial system anti-thrombotic. Surprisingly, use of ACE inhibitors and statins has already been tried in field studies which have suggested they might help humans infected with EBOV[90]. Along these lines, another potentially useful drug is Prostaglandin I_2 (PGI_2, or epoprostenol, its drug name), a powerful vasodilator and anti-coagulant that acts by binding to the prostacyclin receptor. This has potential for use in human filovirus infections to emulate the physiological conditions (low blood pressure and coagulation) in bats that we believe have protective effects[91].

In Infected bats, high HAMP expression seems decoupled from the levels of iron, which should normally be depressed by HAMP. This suggests HAMP inhibitors, used to treat anemia, might prove useful in filoviral infections. Two Hamp inhibitors, Heparin[92] and erythropoietin (EPO) [93,94], have additional effects, anti-coagulation and RBC synthesis respectively, which might make them particularly useful. Vitamin D is also a HAMP inhibitor which could be used with minimal side-effects.

A limitation of our study is our inability to conduct genetic manipulations that would help tease out details of interactions that we have uncovered here. Another limitation is our inability to pursue potential therapeutic agents we have identified. Investigating these effects further requires either reconstituting systems in vitro or experimenting on live animal models, both of which are beyond the scope of this work.

CONCLUSIONS

Bats are an ideal model system for research into the pathobiology of filovirus infection. The resistance of bats to clinical illness provides a useful basis for comparison to human infection. Based on transcriptional analyses, we have composed a framework for understanding a filovirus-infected bat's remarkable resilience to serious

bioRxiv preprint doi: https://doi.org/10.1101/2020.04.13.039503; this version posted April 15, 2020. The copyright holder for this preprint (which was not certified by peer review) is the author/funder, who has granted bioRxiv a license to display the preprint in perpetuity. It is made available under aCC-BY 4.0 International license.

disease, with induction of anti-inflammatory state to be one of the most striking observations. Our study identifies several ways in which the systemic responses in bats and humans to filoviruses differ. These studies have the potential to aid in the development of new strategies to effectively treat filovirus infections in humans.

Data

All data underlying the balloon plots is available as csv files on the shiny tool website (http://katahdin.girihlet.com/shiny/bat/). Additionally, a fasta file containing all the mRNA sequences used in our analysis is available. The raw sequencing reads will be deposited with GEO, and the shiny site has several tools for analysis and exploration of data.

ACKNOWLEDGEMENTS

Oliver Fregoso provided many insightful comments, suggestions, and encouragement for our approach. Viviana Simon and Stu Aaronson read early versions of the manuscript and gave many useful suggestions and encouragement. Ivan V. Kuzmin performed some of the early bat work and provided some critical comments. Radhika Patnala of Sci-Illustrate drew many of the figures. This work was primarily funded by the grant HDTRA1-16-1-0033 from the Defense Threat Reduction Agency.

REFERENCES

1. Messaoudi, I., Amarasinghe, G. K. & Basler, C. F. Filovirus pathogenesis and immune evasion: insights from Ebola virus and Marburg virus. *Nat. Rev. Microbiol.* **13**, 663–676 (2015).
2. Rougeron, V., Feldmann, H., Grard, G., Becker, S. & Leroy, E. M. Ebola and Marburg haemorrhagic fever. *J. Clin. Virol.* **64**, 111–119 (2015).
3. Spengler, J. R., Ervin, E. D., Towner, J. S., Rollin, P. E. & Nichol, S. T. Perspectives on West Africa Ebola Virus Disease Outbreak, 2013-2016. *Emerging Infect. Dis.* **22**, 956–963 (2016).
4. WHO. Ebola health update - DRC, 2019. https://www.who.int/emergencies/diseases/ebola/drc-2019.
5. CDC, M. Outbreak Table | Marburg Hemorrhagic Fever | CDC. https://www.cdc.gov/vhf/marburg/resources/outbreak-table.html.
6. Towner, J. S. *et al.* Isolation of genetically diverse Marburg viruses from Egyptian fruit bats. *PLoS Pathog* **5**, e1000536 (2009).
7. Amman, B. R. *et al.* Seasonal pulses of Marburg virus circulation in juvenile Rousettus aegyptiacus bats coincide with periods of increased risk of human infection. *PLoS Pathog.* **8**, e1002877 (2012).
8. Amman, B. R. *et al.* Isolation of Angola-like Marburg virus from Egyptian rousette bats from West Africa. *Nat Commun* **11**, 510 (2020).
9. Schuh, A. J. *et al.* Modelling filovirus maintenance in nature by experimental transmission of Marburg virus between Egyptian rousette bats. *Nat Commun* **8**, 14446 (2017).
10. Leroy, E. M. *et al.* Human Ebola outbreak resulting from direct exposure to fruit bats in Luebo, Democratic Republic of Congo, 2007. *Vector Borne Zoonotic Dis.* **9**, 723–728 (2009).
11. Marí Saéz, A. *et al.* Investigating the zoonotic origin of the West African Ebola epidemic. *EMBO Mol Med* **7**, 17–23 (2015).
12. Schuh, A. J., Amman, B. R. & Towner, J. S. Filoviruses and bats. *Microbiol. Aust.* **38**, 12–16 (2017).

bioRxiv preprint doi: https://doi.org/10.1101/2020.04.13.039503; this version posted April 15, 2020. The copyright holder for this preprint (which was not certified by peer review) is the author/funder, who has granted bioRxiv a license to display the preprint in perpetuity. It is made available under aCC-BY 4.0 International license.

13. Goldstein, T. *et al.* The discovery of Bombali virus adds further support for bats as hosts of ebolaviruses. *Nat Microbiol* **3**, 1084–1089 (2018).

14. Forbes, K. M. *et al.* Bombali Virus in Mops condylurus Bat, Kenya. *Emerging Infect. Dis.* **25**, (2019).

15. Kemenesi, G. *et al.* Re-emergence of Lloviu virus in Miniopterus schreibersii bats, Hungary, 2016. *Emerg Microbes Infect* **7**, 66 (2018).

16. Negredo, A. *et al.* Discovery of an ebolavirus-like filovirus in europe. *PLoS Pathog.* **7**, e1002304 (2011).

17. Yang, X.-L. *et al.* Characterization of a filovirus (Měnglà virus) from Rousettus bats in China. *Nat Microbiol* **4**, 390–395 (2019).

18. Paweska, J. T. *et al.* Virological and Serological Findings in Rousettus aegyptiacus Experimentally Inoculated with Vero Cells-Adapted Hogan Strain of Marburg Virus. *PLoS One* **7**, (2012).

19. Amman, B. R. *et al.* Oral shedding of Marburg virus in experimentally infected Egyptian fruit bats (Rousettus aegyptiacus). *J. Wildl. Dis.* **51**, 113–124 (2015).

20. Paweska, J. T. *et al.* Lack of Marburg Virus Transmission From Experimentally Infected to Susceptible In-Contact Egyptian Fruit Bats. *J. Infect. Dis.* **212 Suppl 2**, S109-118 (2015).

21. Jones, M. E. B. *et al.* Experimental Inoculation of Egyptian Rousette Bats (Rousettus aegyptiacus) with Viruses of the Ebolavirus and Marburgvirus Genera. *Viruses* **7**, 3420–3442 (2015).

22. Jones, M. E. B. *et al.* Clinical, Histopathologic, and Immunohistochemical Characterization of Experimental Marburg Virus Infection in A Natural Reservoir Host, the Egyptian Rousette Bat (Rousettus aegyptiacus). *Viruses* **11**, (2019).

23. Schuh, A. J. *et al.* Egyptian rousette bats maintain long-term protective immunity against Marburg virus infection despite diminished antibody levels. *Sci Rep* **7**, 8763 (2017).

24. Yuan, J. *et al.* Serological evidence of ebolavirus infection in bats, China. *Virol. J.* **9**, 236 (2012).

25. Olival, K. J. *et al.* Ebola virus antibodies in fruit bats, bangladesh. *Emerging Infect. Dis.* **19**, 270–273 (2013).

26. Pourrut, X. *et al.* Large serological survey showing cocirculation of Ebola and Marburg viruses in Gabonese bat populations, and a high seroprevalence of both viruses in Rousettus aegyptiacus. *BMC Infect. Dis.* **9**, 159 (2009).

27. Krähling, V. *et al.* Establishment of fruit bat cells (Rousettus aegyptiacus) as a model system for the investigation of filoviral infection. *PLoS Negl Trop Dis* **4**, e802 (2010).

28. Jebb, D. *et al.* Six new reference-quality bat genomes illuminate the molecular basis and evolution of bat adaptations. *bioRxiv* 836874 (2019) doi:10.1101/836874.

29. Kuzmin, I. V. *et al.* Innate Immune Responses of Bat and Human Cells to Filoviruses: Commonalities and Distinctions. *J. Virol.* **91**, (2017).

30. Albariño, C. G. *et al.* Development of a reverse genetics system to generate recombinant Marburg virus derived from a bat isolate. *Virology* **446**, 230–237 (2013).

31. Bray, N. L., Pimentel, H., Melsted, P. & Pachter, L. Near-optimal probabilistic RNA-seq quantification. *Nature Biotechnology* **34**, 525–527 (2016).

32. Hölzer, M. *et al.* Differential transcriptional responses to Ebola and Marburg virus infection in bat and human cells. *Scientific Reports* **6**, 34589 (2016).

33. Becker, S., Spiess, M. & Klenk, H. D. The asialoglycoprotein receptor is a potential liver-specific receptor for Marburg virus. *J. Gen. Virol.* **76 (Pt 2)**, 393–399 (1995).

34. Kushner, I. The phenomenon of the acute phase response. *Ann. N. Y. Acad. Sci.* **389**, 39–48 (1982).

bioRxiv preprint doi: https://doi.org/10.1101/2020.04.13.039503; this version posted April 15, 2020. The copyright holder for this preprint (which was not certified by peer review) is the author/funder, who has granted bioRxiv a license to display the preprint in perpetuity. It is made available under aCC-BY 4.0 International license.

35. Gabay, C. & Kushner, I. Acute-phase proteins and other systemic responses to inflammation. *N. Engl. J. Med.* **340**, 448–454 (1999).

36. Gauldie, J., Richards, C., Harnish, D., Lansdorp, P. & Baumann, H. Interferon beta 2/B-cell stimulatory factor type 2 shares identity with monocyte-derived hepatocyte-stimulating factor and regulates the major acute phase protein response in liver cells. *Proc. Natl. Acad. Sci. U.S.A.* **84**, 7251–7255 (1987).

37. Moshage, H. J., Janssen, J. A., Franssen, J. H., Hafkenscheid, J. C. & Yap, S. H. Study of the molecular mechanism of decreased liver synthesis of albumin in inflammation. *J. Clin. Invest.* **79**, 1635–1641 (1987).

38. Kushner, I. Acute phase reactants. *UpToDate* https://www.uptodate.com/contents/acute-phase-reactants.

39. Gabay, C., Smith, M. F., Eidlen, D. & Arend, W. P. Interleukin 1 receptor antagonist (IL-1Ra) is an acute-phase protein. *J. Clin. Invest.* **99**, 2930–2940 (1997).

40. Loyer, P. *et al.* Interleukin 4 inhibits the production of some acute-phase proteins by human hepatocytes in primary culture. *FEBS Lett.* **336**, 215–220 (1993).

41. Mackiewicz, A., Schooltink, H., Heinrich, P. C. & Rose-John, S. Complex of soluble human IL-6-receptor/IL-6 up-regulates expression of acute-phase proteins. *J. Immunol.* **149**, 2021–2027 (1992).

42. Dvash, E., Har-Tal, M., Barak, S., Meir, O. & Rubinstein, M. Leukotriene C 4 is the major trigger of stress-induced oxidative DNA damage. *Nat Commun* **6**, 1–15 (2015).

43. Mahanty, S. & Bray, M. Pathogenesis of filoviral haemorrhagic fevers. *The Lancet Infectious Diseases* **4**, 487–498 (2004).

44. Rőszer, T. Understanding the Mysterious M2 Macrophage through Activation Markers and Effector Mechanisms. *Mediators Inflamm.* **2015**, 816460 (2015).

45. Ferrante, C. J. *et al.* The adenosine-dependent angiogenic switch of macrophages to an M2-like phenotype is independent of interleukin-4 receptor alpha (IL-4Rα) signaling. *Inflammation* **36**, 921–931 (2013).

46. Atri, C., Guerfali, F. Z. & Laouini, D. Role of Human Macrophage Polarization in Inflammation during Infectious Diseases. *Int J Mol Sci* **19**, (2018).

47. Parisi, L. *et al.* Macrophage Polarization in Chronic Inflammatory Diseases: Killers or Builders? *J Immunol Res* **2018**, (2018).

48. Helming, L. Inflammation: Cell Recruitment versus Local Proliferation. *Current Biology* **21**, R548–R550 (2011).

49. Jenkins, S. J. *et al.* Local macrophage proliferation, rather than recruitment from the blood, is a signature of TH2 inflammation. *Science* **332**, 1284–1288 (2011).

50. Raggi, F. *et al.* Regulation of Human Macrophage M1–M2 Polarization Balance by Hypoxia and the Triggering Receptor Expressed on Myeloid Cells-1. *Front Immunol* **8**, (2017).

51. Krawczyk, C. M. *et al.* Toll-like receptor-induced changes in glycolytic metabolism regulate dendritic cell activation. *Blood* **115**, 4742–4749 (2010).

52. Tannahill, G. M. *et al.* Succinate is an inflammatory signal that induces IL-1β through HIF-1α. *Nature* **496**, 238–242 (2013).

53. Nizet, V. & Johnson, R. S. Interdependence of hypoxic and innate immune responses. *Nat. Rev. Immunol.* **9**, 609–617 (2009).

54. Tan, Z. *et al.* Pyruvate dehydrogenase kinase 1 participates in macrophage polarization via regulating glucose metabolism. *J. Immunol.* **194**, 6082–6089 (2015).

55. Imamura, R. & Matsumoto, K. Hepatocyte growth factor in physiology and infectious diseases. *Cytokine* **98**, 97–106 (2017).

bioRxiv preprint doi: https://doi.org/10.1101/2020.04.13.039503; this version posted April 15, 2020. The copyright holder for this preprint (which was not certified by peer review) is the author/funder, who has granted bioRxiv a license to display the preprint in perpetuity. It is made available under aCC-BY 4.0 International license.

56. Agoro, R., Taleb, M., Quesniaux, V. F. J. & Mura, C. Cell iron status influences macrophage polarization. *PLOS ONE* **13**, e0196921 (2018).

57. Murphy, M. P. Rerouting metabolism to activate macrophages. *Nat Immunol* 1–3 (2019) doi:10.1038/s41590-019-0455-5.

58. Noris, M. & Remuzzi, G. Overview of Complement Activation and Regulation. *Semin Nephrol* **33**, 479–492 (2013).

59. Schuh, A. J. *et al.* Antibody-Mediated Virus Neutralization Is Not a Universal Mechanism of Marburg, Ebola, or Sosuga Virus Clearance in Egyptian Rousette Bats. *J. Infect. Dis.* **219**, 1716–1721 (2019).

60. McElroy, A. K. *et al.* Human Ebola virus infection results in substantial immune activation. *Proc. Natl. Acad. Sci. U.S.A.* **112**, 4719–4724 (2015).

61. Dahlke, C. *et al.* Comprehensive Characterization of Cellular Immune Responses Following Ebola Virus Infection. *J. Infect. Dis.* **215**, 287–292 (2017).

62. Reynard, S. *et al.* Immune parameters and outcomes during Ebola virus disease. *JCI Insight* **4**, (2019).

63. Knutson, M. D. Iron transport proteins: Gateways of cellular and systemic iron homeostasis. *J. Biol. Chem.* **292**, 12735–12743 (2017).

64. Przybyszewska, J. & Żekanowska, E. The role of hepcidin, ferroportin, HCP1, and DMT1 protein in iron absorption in the human digestive tract. *Prz Gastroenterol* **9**, 208–213 (2014).

65. Prentice, A. M. *et al.* Hepcidin is the major predictor of erythrocyte iron incorporation in anemic African children. *Blood* **119**, 1922–1928 (2012).

66. Michels, K., Nemeth, E., Ganz, T. & Mehrad, B. Hepcidin and Host Defense against Infectious Diseases. *PLoS Pathog* **11**, (2015).

67. Wessling-Resnick, M. Crossing the Iron Gate: Why and How Transferrin Receptors Mediate Viral Entry. *Annu. Rev. Nutr.* **38**, 431–458 (2018).

68. Kohgo, Y., Ikuta, K., Ohtake, T., Torimoto, Y. & Kato, J. Body iron metabolism and pathophysiology of iron overload. *Int J Hematol* **88**, 7–15 (2008).

69. Gao, G. & Chang, Y.-Z. Mitochondrial ferritin in the regulation of brain iron homeostasis and neurodegenerative diseases. *Front Pharmacol* **5**, (2014).

70. Yanatori, I. & Kishi, F. DMT1 and iron transport. *Free Radic. Biol. Med.* **133**, 55–63 (2019).

71. Sendamarai, A. K., Ohgami, R. S., Fleming, M. D. & Lawrence, C. M. Structure of the membrane proximal oxidoreductase domain of human Steap3, the dominant ferrireductase of the erythroid transferrin cycle. *PNAS* **105**, 7410–7415 (2008).

72. Brown, N. J. & Vaughan, D. E. Role of Angiotensin II in Coagulation and Fibrinolysis. *Heart Fail Rev* **3**, 193–198 (1999).

73. Conway, E. M. Complement-coagulation connections. *Blood Coagulation & Fibrinolysis* **29**, 243 (2018).

74. Feldmann, H. & Klenk, H.-D. Filoviruses. in *Medical Microbiology* (ed. Baron, S.) (University of Texas Medical Branch at Galveston, 1996).

75. Zhou, P. *et al.* Contraction of the type I IFN locus and unusual constitutive expression of IFN-α in bats. *Proc. Natl. Acad. Sci. U.S.A.* **113**, 2696–2701 (2016).

76. Glennon, N. B., Jabado, O., Lo, M. K. & Shaw, M. L. Transcriptome Profiling of the Virus-Induced Innate Immune Response in Pteropus vampyrus and Its Attenuation by Nipah Virus Interferon Antagonist Functions. *J. Virol.* **89**, 7550–7566 (2015).

77. Pavlovich, S. S. *et al.* The Egyptian Rousette Genome Reveals Unexpected Features of Bat Antiviral Immunity. *Cell* **173**, 1098-1110.e18 (2018).

bioRxiv preprint doi: https://doi.org/10.1101/2020.04.13.039503; this version posted April 15, 2020. The copyright holder for this preprint (which was not certified by peer review) is the author/funder, who has granted bioRxiv a license to display the preprint in perpetuity. It is made available under aCC-BY 4.0 International license.

78. Xie, J. *et al.* Dampened STING-Dependent Interferon Activation in Bats. *Cell Host Microbe* **23**, 297-301.e4 (2018).

79. Maringer, K. & Fernandez-Sesma, A. Message in a bottle: lessons learned from antagonism of STING signalling during RNA virus infection. *Cytokine & Growth Factor Reviews* **25**, 669–679 (2014).

80. Franz, K. M., Neidermyer, W. J., Tan, Y.-J., Whelan, S. P. J. & Kagan, J. C. STING-dependent translation inhibition restricts RNA virus replication. *Proc. Natl. Acad. Sci. U.S.A.* **115**, E2058–E2067 (2018).

81. Holm, C. K. *et al.* Influenza A virus targets a cGAS-independent STING pathway that controls enveloped RNA viruses. *Nat Commun* **7**, 10680 (2016).

82. Liu, X. *et al.* Transcriptomic signatures differentiate survival from fatal outcomes in humans infected with Ebola virus. *Genome Biology* **18**, 4 (2017).

83. McElroy, A. K. *et al.* Ebola hemorrhagic Fever: novel biomarker correlates of clinical outcome. *J. Infect. Dis.* **210**, 558–566 (2014).

84. Leligdowicz, A. *et al.* Ebola virus disease and critical illness. *Crit Care* **20**, 217 (2016).

85. Guo Liang, Sakamoto Atsushi, Cornelissen Anne, Hong Charles C. & Finn Aloke V. Ironing-Out the Role of Hepcidin in Atherosclerosis. *Arteriosclerosis, Thrombosis, and Vascular Biology* **39**, 303–305 (2019).

86. Livesey, J. A. *et al.* Low serum iron levels are associated with elevated plasma levels of coagulation factor VIII and pulmonary emboli/deep venous thromboses in replicate cohorts of patients with hereditary haemorrhagic telangiectasia. *Thorax* **67**, 328–333 (2012).

87. Zhang, H. *et al.* TMEM173 Drives Lethal Coagulation in Sepsis. *Cell Host & Microbe* **0**, (2020).

88. Younan, P., Ramanathan, P., Graber, J., Gusovsky, F. & Bukreyev, A. The Toll-Like Receptor 4 Antagonist Eritoran Protects Mice from Lethal Filovirus Challenge. *MBio* **8**, (2017).

89. Fedson, D. S. A Practical Treatment for Patients With Ebola Virus Disease. *J Infect Dis* **211**, 661–662 (2015).

90. Fedson, D. S. & Rordam, O. M. Treating Ebola patients: a 'bottom up' approach using generic statins and angiotensin receptor blockers. *International Journal of Infectious Diseases* **36**, 80–84 (2015).

91. Cacione, D. G., Macedo, C. R. & Baptista-Silva, J. C. Pharmacological treatment for Buerger's disease. *Cochrane Database of Systematic Reviews* (2016) doi:10.1002/14651858.CD011033.pub3.

92. Poli, M. *et al.* Heparin: a potent inhibitor of hepcidin expression in vitro and in vivo. *Blood* **117**, 997–1004 (2011).

93. Arezes, J. *et al.* Erythroferrone inhibits the induction of hepcidin by BMP6. *Blood* **132**, 1473–1477 (2018).

94. Nai, A. *et al.* Limiting hepatic Bmp-Smad signaling by matriptase-2 is required for erythropoietin-mediated hepcidin suppression in mice. *Blood* **127**, 2327–2336 (2016).

95. Jones, S. A., Scheller, J. & Rose-John, S. Therapeutic strategies for the clinical blockade of IL-6/gp130 signaling. *J Clin Invest* **121**, 3375–3383 (2011).

96. Schoels, M. M. *et al.* Blocking the effects of interleukin-6 in rheumatoid arthritis and other inflammatory rheumatic diseases: systematic literature review and meta-analysis informing a consensus statement. *Ann Rheum Dis* **72**, 583–589 (2013).

bioRxiv preprint doi: https://doi.org/10.1101/2020.04.13.039503; this version posted April 15, 2020. The copyright holder for this preprint (which was not certified by peer review) is the author/funder, who has granted bioRxiv a license to display the preprint in perpetuity. It is made available under aCC-BY 4.0 International license.

Figures

Underlying data and tools for exploring the data available at http://katahdin.girihlet.com/shiny/bat/

bioRxiv preprint doi: https://doi.org/10.1101/2020.04.13.039503; this version posted April 15, 2020. The copyright holder for this preprint (which was not certified by peer review) is the author/funder, who has granted bioRxiv a license to display the preprint in perpetuity. It is made available under aCC-BY 4.0 International license.

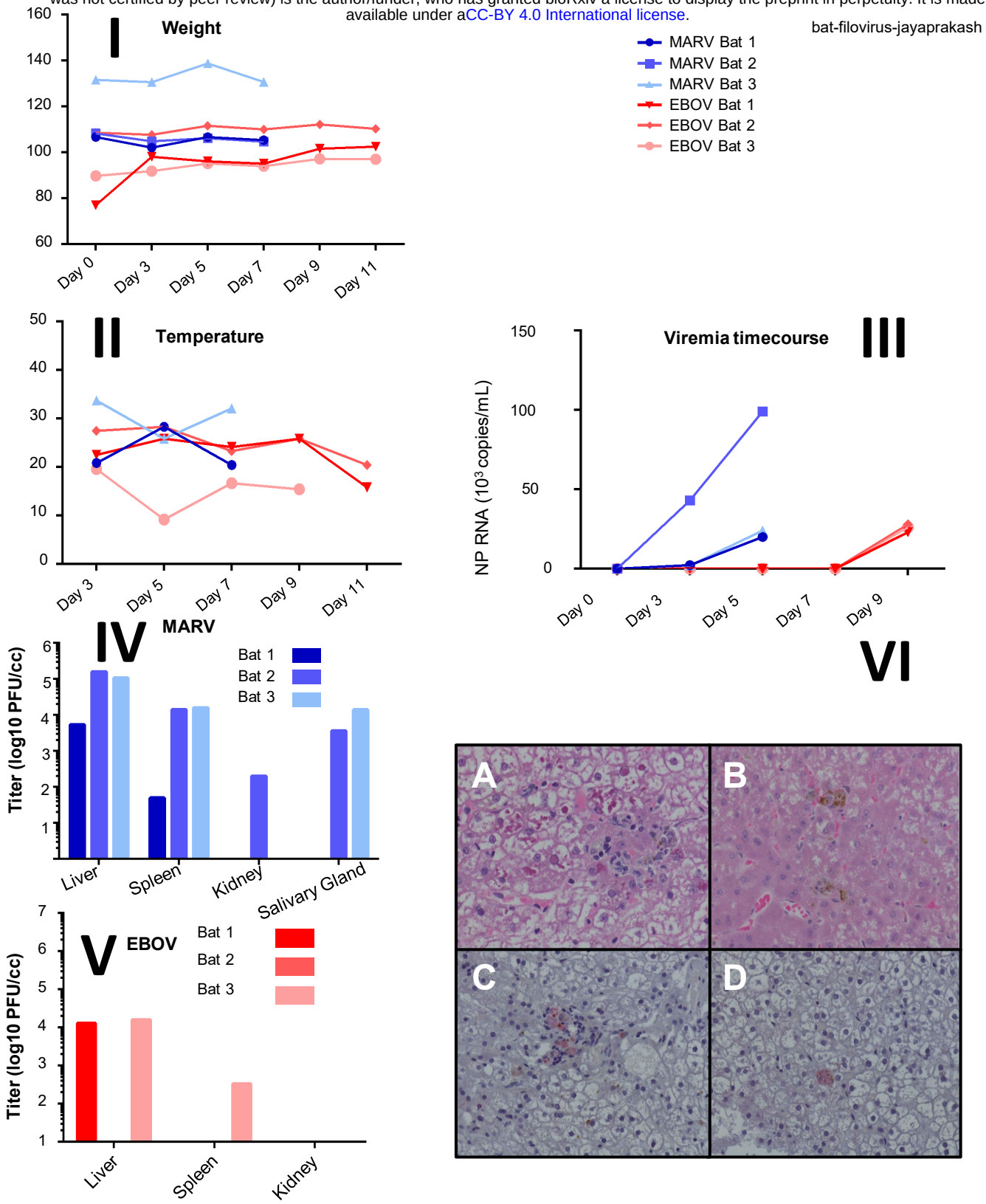

Figure 1: Bat infection with filovirus, MARV and EBOV. Time course after infection for I) Weight**, II)** temperature and **III)** viremia (MARV Bat 2 sensor failed). Viremia measured in total RNA extracted from whole blood via ddRT-PCR targeting the viral NP gene. Animals were euthanized 48 hours after last viremic timepoint. **Tissue viral loads (IV and V)** were determined by conventional plaque assay on Vero E6 cells. **V1) Histopathology in EBOV infected livers showing VI.A)** EBOV Bat 1 liver with marked histopathological changes, including cytoplasmic and nuclear inclusions**, V1. B.)** EBOV Bat 2 liver displaying a less dramatic presentation compared to Bat 1, **V1.C)** IHC detection of filovirus antigen in EBOV Bat 1 liver, and **V1. D.)** IHC detection of EBOV VP40 in EBOV Bat 1 liver.

bioRxiv preprint doi: https://doi.org/10.1101/2020.04.13.039503; this version posted April 15, 2020. The copyright holder for this preprint (which was not certified by peer review) is the author/funder, who has granted bioRxiv a license to display the preprint in perpetuity. It is made available under aCC-BY 4.0 International license.

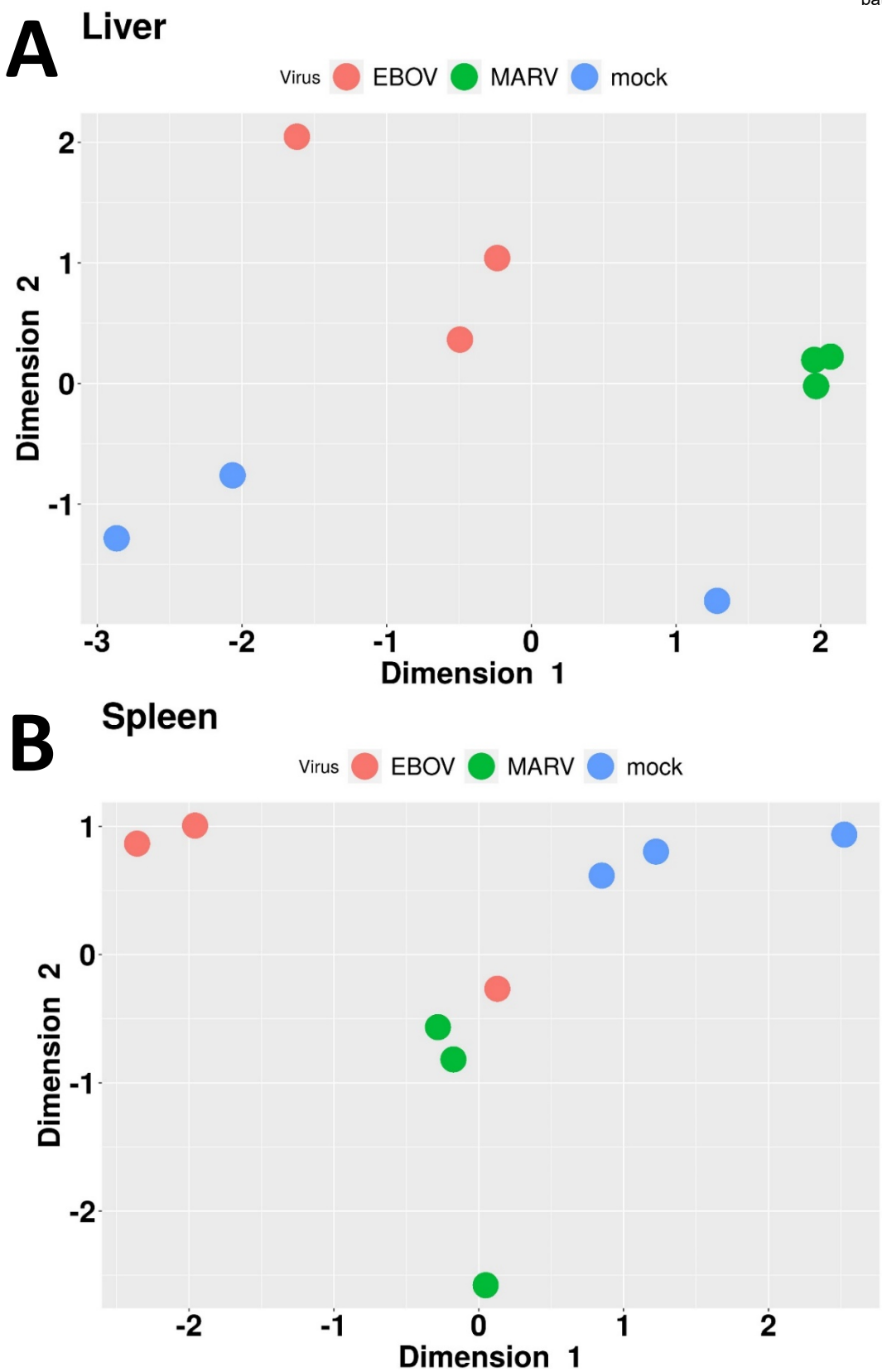

Figure 2: MDS plots along the two leading dimensions (the x and y axis respectively). There is clear separation between different infections (MARV and EBOV) and the mock-infected samples in Liver (**A**) and Spleen (**B**). Despite the paucity of viral transcripts, Spleen and other tissues (PBMC, kidney, salivary gland, lung, large and small intestine, **Fig. S1**) also exhibit virus-specific signatures, implying the response to filovirus infections extends to the whole organism (system) in bats. The left panel has an outlier uninfected liver sample (the lower-right blue sample) which has been excluded in the analysis.

bioRxiv preprint doi: https://doi.org/10.1101/2020.04.13.039503; this version posted April 15, 2020. The copyright holder for this preprint (which was not certified by peer review) is the author/funder, who has granted bioRxiv a license to display the preprint in perpetuity. It is made available under aCC-BY 4.0 International license.

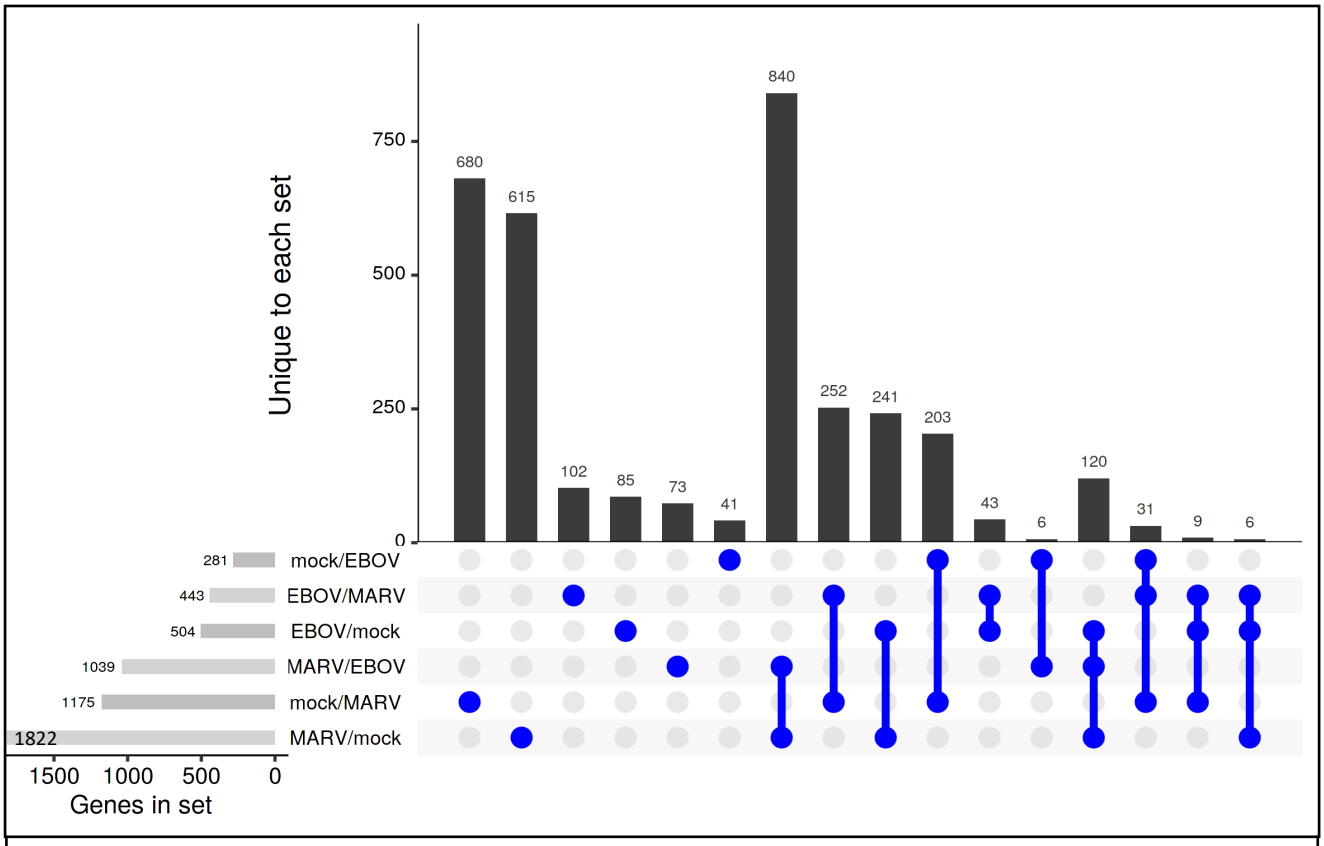

Figure 3: Upset plot for data from bat liver. Upset plots are an alternative to complex Venn diagrams. In the plot, *mock* refers to mock-infected bats, *EBOV* to EBOV-infected bats, and *MARV* to MARV-infected bat livers. Each row in the lower panel represents a set, with the corresponding colored bars at the lower left representing membership in the sets. There are six sets of genes, *EBOV/mock* comprises of genes at least 2-fold up regulated in EBOV infection, compared to the mock samples, while *mock/EBOV* is genes at least 2-fold down regulated in EBOV samples compared to the mock samples. The vertical blue lines with bulbs represent set intersections, the main bar plot (top) is number of genes unique to that intersection, so the total belonging to a set, say mock/EBOV, is a sum of the numbers in all sets that have mock/EBOV as a member (41+203+6+31=281). For example, the last bar is the set of genes common to *EBOV/MARV*, *EBOV/mock* and *MARV/mock,* so are up 2-fold in EBOV compared to the *mock* and *MARV* samples, and at least 2-fold up in *MARV* compared to *mock*. Many more genes respond to infection by MARV than by EBOV. The EBOV-specific (*EBOV/MARV)* and MARV-specific (*MARV/EBOV)* genes are likely host responses specific to the viral VP40, VP35 and VP24 genes.

bioRxiv preprint doi: https://doi.org/10.1101/2020.04.13.039503; this version posted April 15, 2020. The copyright holder for this preprint (which was not certified by peer review) is the author/funder, who has granted bioRxiv a license to display the preprint in perpetuity. It is made available under aCC-BY 4.0 International license.

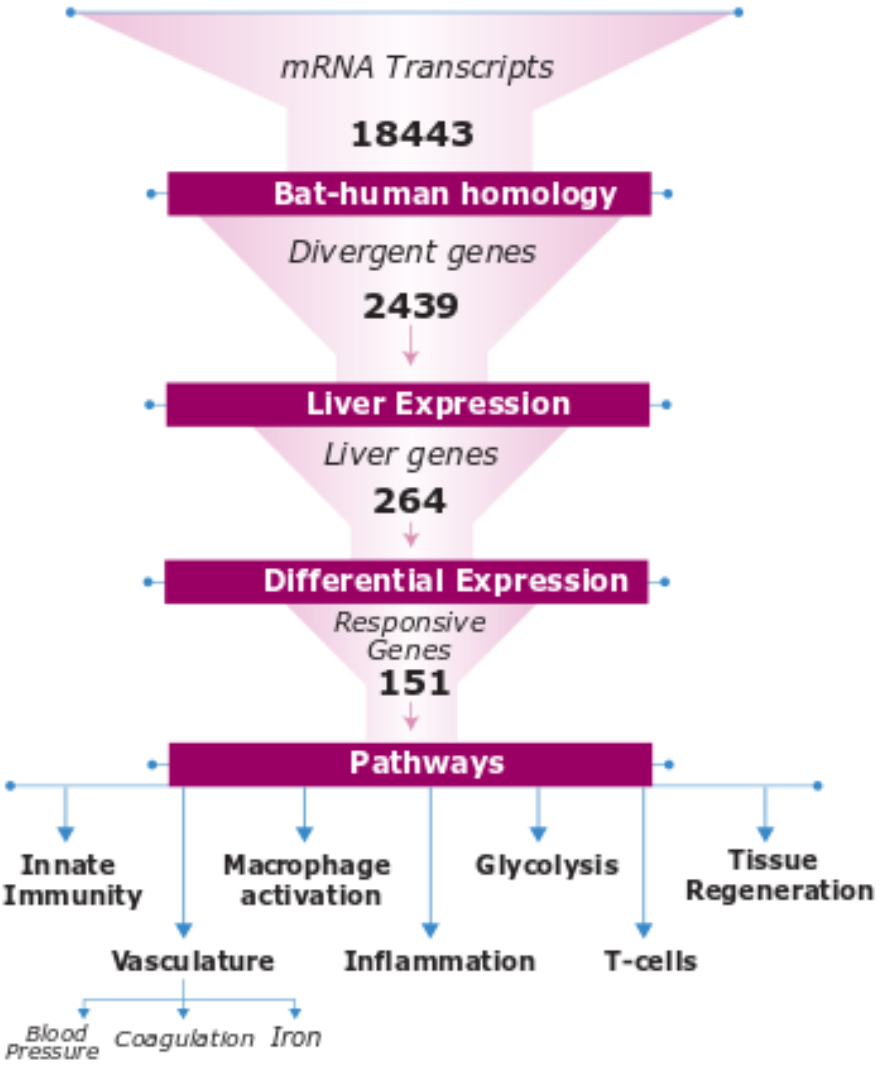

Figure 4. Genes to Pathways. The process used in the paper to identify pathways of interest to help explain the bat's resilience in the face of filoviral infection. Bat genes evolutionarily divergent from their human homologs that are responsive in liver to filovirus infection were identified. The pathways they participate in were explored to understand the systemic response to filovirus infections in bats and identify key differences from human responses. The vascular system (Blood pressure, Coagulation and Iron homeostasis) was a prominent pathway. Glycolysis, which is controlled by Hypoxia, is responsible for the balance between M1 and M2 states of macrophage activation. The pathways are interconnected, as we show in subsequent figures.

bioRxiv preprint doi: https://doi.org/10.1101/2020.04.13.039503; this version posted April 15, 2020. The copyright holder for this preprint (which was not certified by peer review) is the author/funder, who has granted bioRxiv a license to display the preprint in perpetuity. It is made available under aCC-BY 4.0 International license.

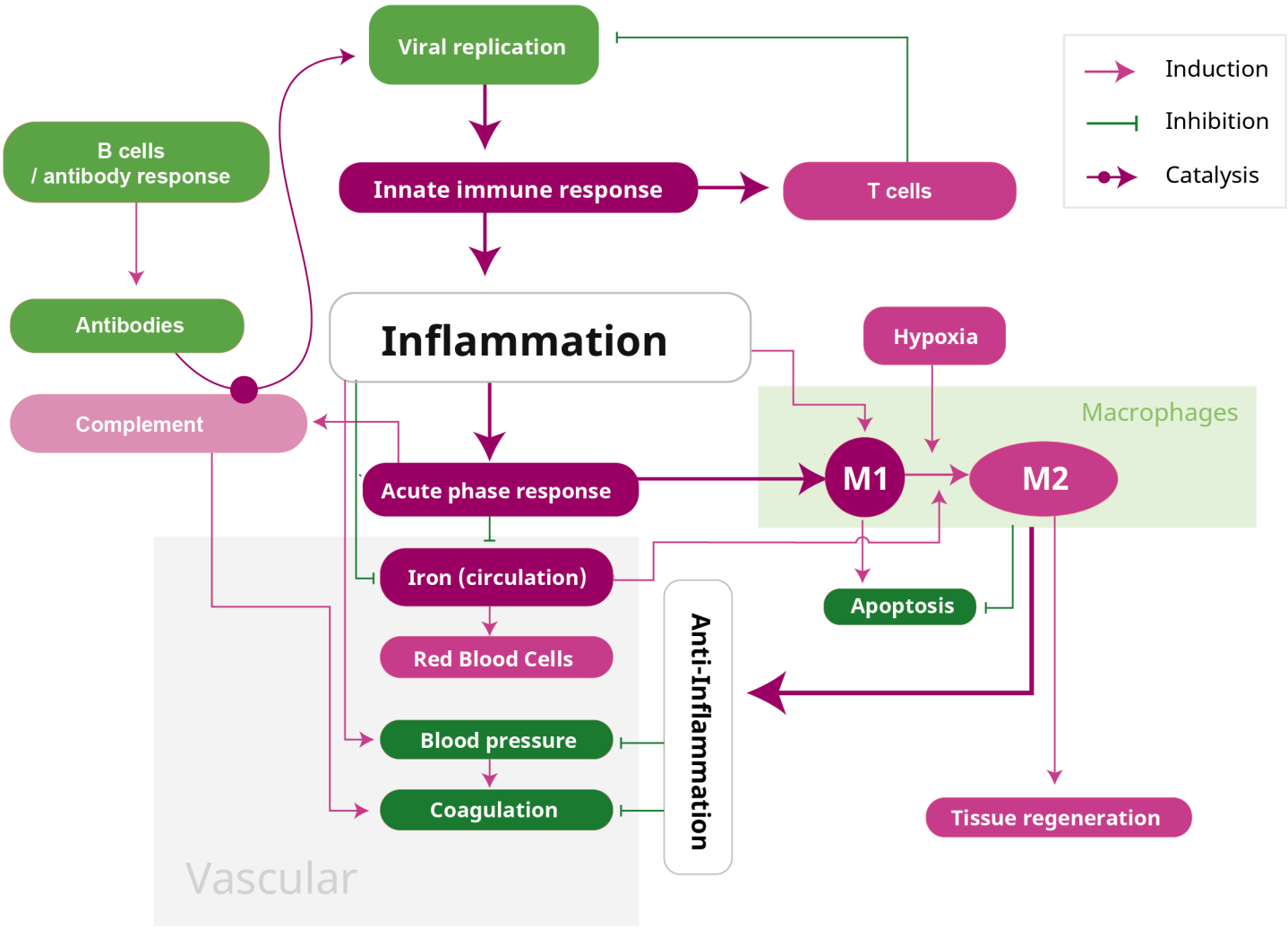

Figure 5: Overview of the pathways/processes triggered by filovirus replication. The innate immune response causes inflammation, which triggers an acute phase response (APR), leading to a cascade of vascular events, affecting regulation of HAMP (iron), coagulation, blood pressure and M1 macrophage stimulation. The anti-inflammatory state characterized by M2 macrophages is increased relative to the M1 macrophages in both EBOV and MARV. M1 to M2 conversions are possible. Coagulation and blood pressure are down regulated in MARV and EBOV infection, while iron levels are high, especially in EBOV infection (contrary to the levels of HAMP). Fatty acid oxidation and mitochondrial activity are up, which are hallmarks of M2 macrophages. T cell (CD8) activity is also upregulated. The complement system is incompletely stimulated by the acute phase response, leading to potentially restricted antibody activity. The details are given in subsequent figures.

bioRxiv preprint doi: https://doi.org/10.1101/2020.04.13.039503; this version posted April 15, 2020. The copyright holder for this preprint (which was not certified by peer review) is the author/funder, who has granted bioRxiv a license to display the preprint in perpetuity. It is made available under aCC-BY 4.0 International license.

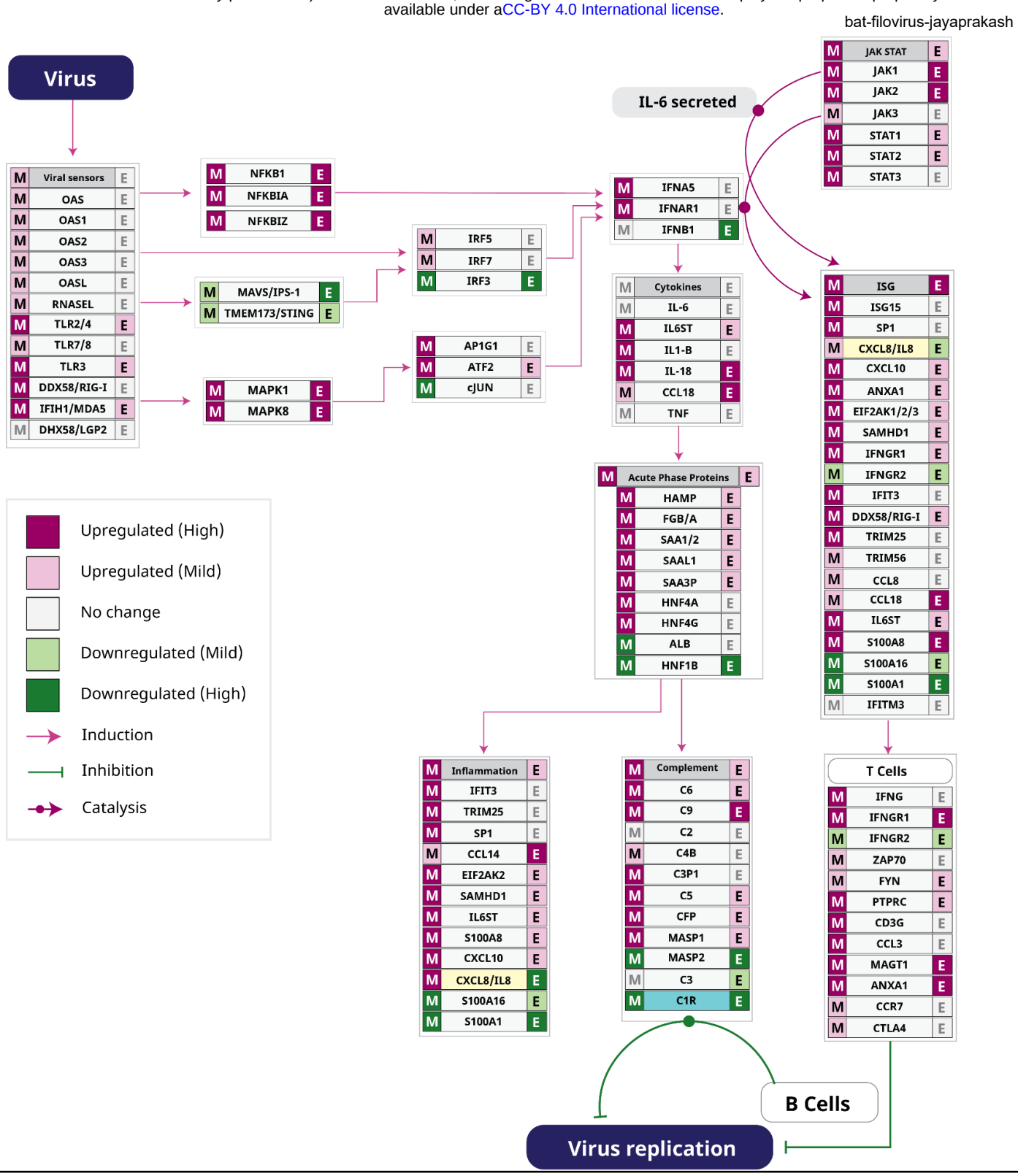

Figure 6: **Innate response to filoviruses.** Virus RNA/proteins are detected by sensors, leading to upregulation of Interferon type I (IFNA and IFNB) and interferon stimulated genes (ISG) through the JAK-STAT pathway. Cytokines chemokines create an anti-viral state in the cell. Inflammation (IL-6) triggers expression of acute phase proteins. Secretion of interferon gamma enables an adaptive immune system response. In human and bat cell lines, interferon responses to the filoviruses were similar. EBOV VP24 inhibits STAT1, while MARV VP40 inhibits JAK1 and filovirus VP35 interferes with IRF3/7, which can lead to filovirus-specific responses e.g. CXCL10 is up/down-regulated/ by MARV/EBOV infection, while CCL18 is upregulated by both, (cell line data). The robust innate response to filovirus infection in bats and humans suggests any constitutive expression of innate response genes in bats is irrelevant. Colored bands (MARV-left and EBOV-right) by gene names depict the effect of filovirus infection on expression.

bioRxiv preprint doi: https://doi.org/10.1101/2020.04.13.039503; this version posted April 15, 2020. The copyright holder for this preprint (which was not certified by peer review) is the author/funder, who has granted bioRxiv a license to display the preprint in perpetuity. It is made available under aCC-BY 4.0 International license.

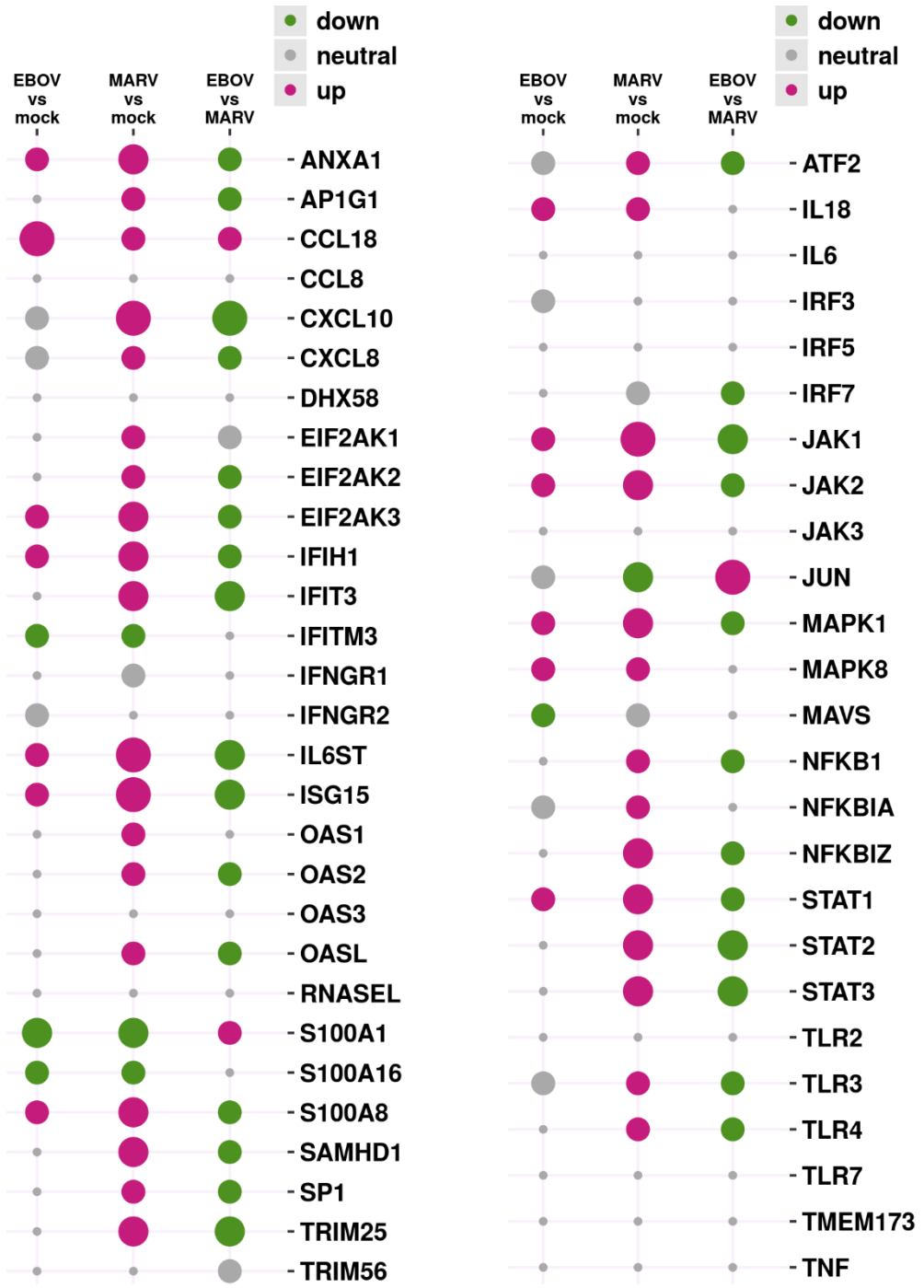

Figure 7: Interferon stimulated genes (ISG). MARV and EBOV elicit a strong innate response driven by Interferons. These responses are also seen in cell line data, with the differences reflecting the interactions of viral VP35, VP40 and VP24 proteins with host proteins, e.g. both cell line and bat data show CXCL10 is upregulated by MARV infection, but not by EBOV infection, while CCL18 is up under both. The balloon plot shows comparisons of responses of ISG genes to EBOV, MARV and mock against each other. The radius of circle is proportional to log2(ratio), gray is used when absolute values of log2(ratio) < 0.6.

bioRxiv preprint doi: https://doi.org/10.1101/2020.04.13.039503; this version posted April 15, 2020. The copyright holder for this preprint (which was not certified by peer review) is the author/funder, who has granted bioRxiv a license to display the preprint in perpetuity. It is made available under aCC-BY 4.0 International license.

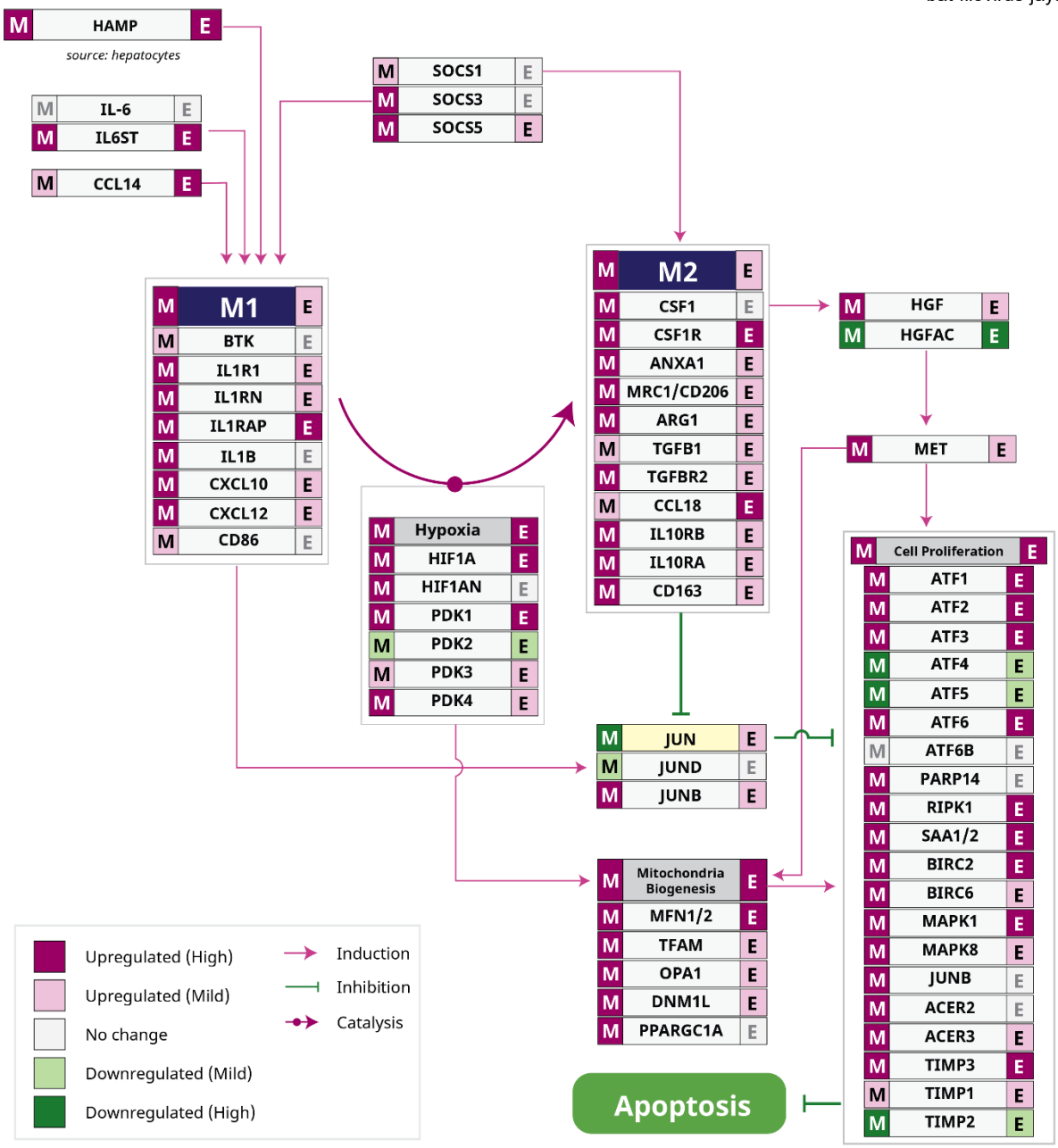

Figure 8: Macrophage polarization during filovirus infections. HAMP induces macrophages in the M1 state. Cell iron status also influences macrophage polarization[54], which leads to vascular effects[80]. During filovirus infection, the system is in an anti-inflammatory state (markers for M2 are up), while during MARV infection, the inflammatory M1 state is also seen, consistent with the acute phase response involving down regulation of albumin and upregulation of SAA1/2.
The M1-M2 switch is anti-inflammatory and promotes wound healing, low-angiotensin, hematopoiesis etc. Different SOCS family molecules are molecular switches that control M1/M2 macrophage polarization. High expression of SOCS3 in MARV infection promotes M1 polarization. M2 markers are also upregulated.
The M2 state is probably the key to the resilience of bats during filovirus infection, allowing bats to fight off filoviruses without significant adverse effects. Under MARV infection, there is limited viral replication and disease symptoms before it is cleared, consistent with this, the anti-inflammatory state is not as pronounced as in the case of EBOV-infected bats. The anti-inflammatory state is also characterized by tissue regeneration, which is facilitated by an increase in mitochondrial numbers and fatty acid oxidation activity. There is also a connection between iron metabolism and macrophage M1/M2 polarization with increasing iron favoring M2[54]. The colored bands on either side of the gene names depict the effect of filovirus infection on expression (MARV-left and EBOV-right).

bioRxiv preprint doi: https://doi.org/10.1101/2020.04.13.039503; this version posted April 15, 2020. The copyright holder for this preprint (which was not certified by peer review) is the author/funder, who has granted bioRxiv a license to display the preprint in perpetuity. It is made available under aCC-BY 4.0 International license.

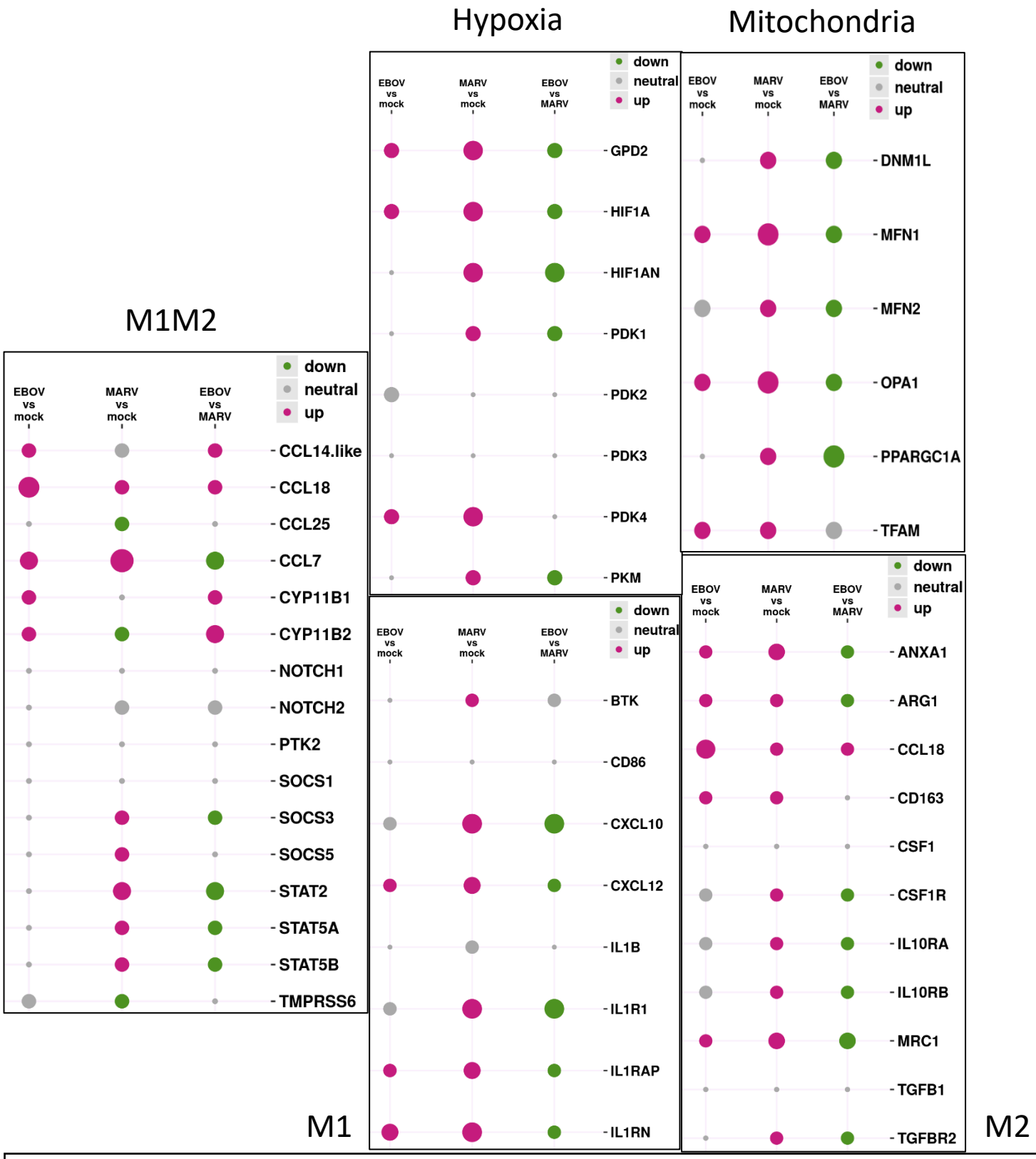

Figure 9: Macrophage activation. Genes specific to the M1 and M2 (bottom right panels) show that M1 and M2 states are activated by filovirus infection with the M1/M2 ratio being higher in MARV infection. The left panel shows genes common to both M1 and M2 states, while the two panels on the top right show genes involved in hypoxia and mitochondrial abundance. The balloon plot shows comparisons of responses of genes to EBOV, MARV and mock against each other. The radius of circle is proportional to log2(ratio), gray is used when absolute values of log2(ratio) < 0.6.

bioRxiv preprint doi: https://doi.org/10.1101/2020.04.13.039503; this version posted April 15, 2020. The copyright holder for this preprint (which was not certified by peer review) is the author/funder, who has granted bioRxiv a license to display the preprint in perpetuity. It is made available under aCC-BY 4.0 International license.

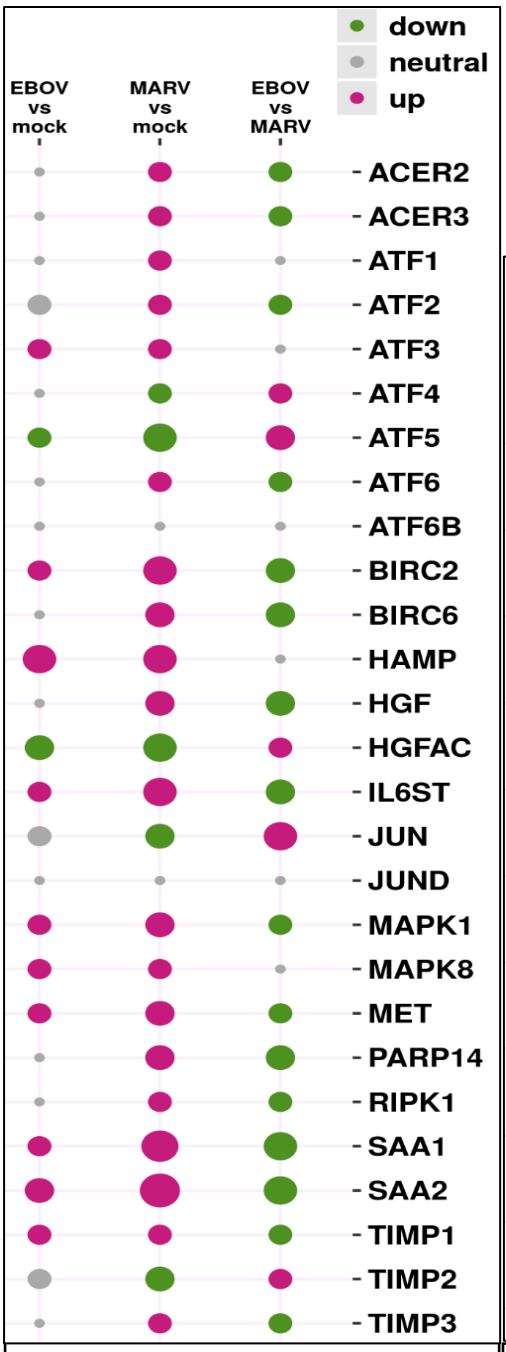

Figure 10: Tissue regeneration. Filovirus infections in bat eventually triggers tissue regeneration, reflected in the M2 macrophages, which are anti-inflammatory. The balloon plot compares responses of genes to EBOV, MARV and mock against each other. The radius of circle is proportional to log2(ratio), gray is used when absolute values of log2(ratio) < 0.6. There is more activity under MARV infection, consistent with higher viral loads.

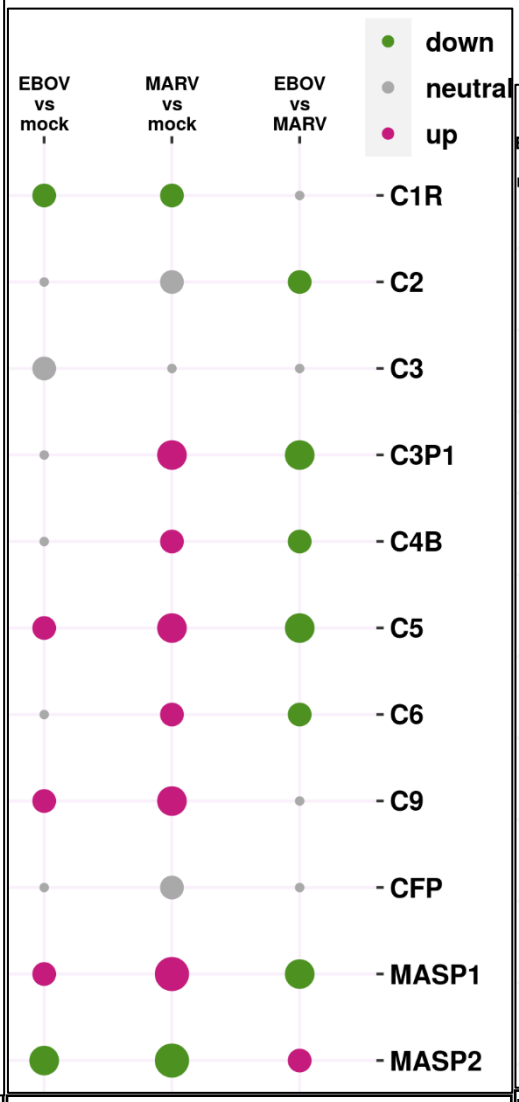

Figure 11: Complement System. C1R, C3 and MASP2 are down regulated by filovirus infection in bats, likely leading to compromised antibody activity. The balloon plot compares responses of genes to EBOV, MARV and mock against each other. The radius of circle is proportional to log2(ratio), gray is used when absolute values of log2(ratio) < 0.6.

Figure 12: CD8 T cell genes. Most are upregulated by filovirus infection, reflecting enhanced CD8 T cell activity, which probably plays a major role in controlling the infections. The balloon plot compares responses of genes to EBOV, MARV and mock against each other. The radius of circle is proportional to log2(ratio), gray is used when absolute values of log2(ratio) < 0.6.

bioRxiv preprint doi: https://doi.org/10.1101/2020.04.13.039503; this version posted April 15, 2020. The copyright holder for this preprint (which was not certified by peer review) is the author/funder, who has granted bioRxiv a license to display the preprint in perpetuity. It is made available under aCC-BY 4.0 International license.

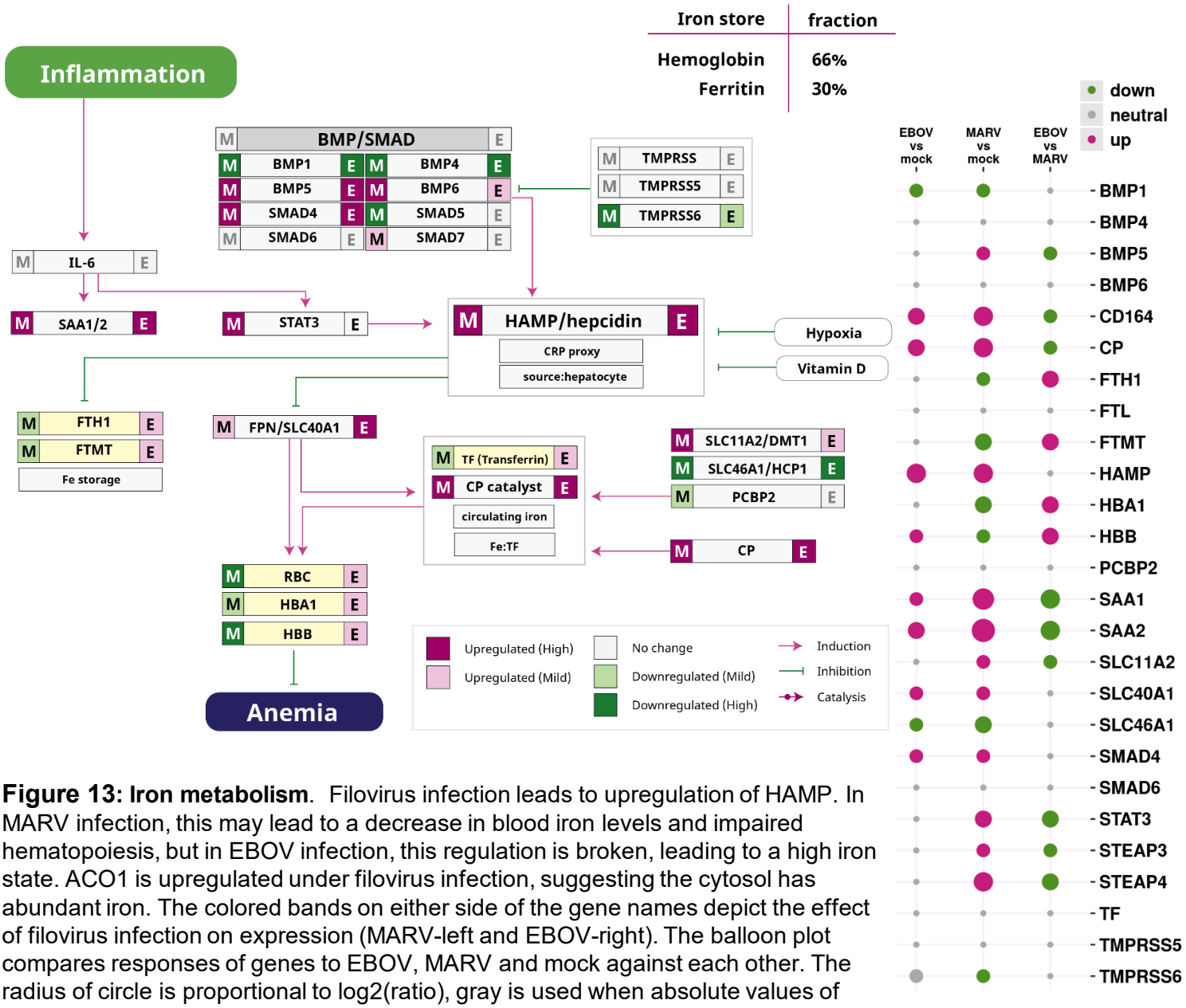

Figure 13: Iron metabolism. Filovirus infection leads to upregulation of HAMP. In MARV infection, this may lead to a decrease in blood iron levels and impaired hematopoiesis, but in EBOV infection, this regulation is broken, leading to a high iron state. ACO1 is upregulated under filovirus infection, suggesting the cytosol has abundant iron. The colored bands on either side of the gene names depict the effect of filovirus infection on expression (MARV-left and EBOV-right). The balloon plot compares responses of genes to EBOV, MARV and mock against each other. The radius of circle is proportional to log2(ratio), gray is used when absolute values of log2(ratio) < 0.6.

bioRxiv preprint doi: https://doi.org/10.1101/2020.04.13.039503; this version posted April 15, 2020. The copyright holder for this preprint (which was not certified by peer review) is the author/funder, who has granted bioRxiv a license to display the preprint in perpetuity. It is made available under aCC-BY 4.0 International license.

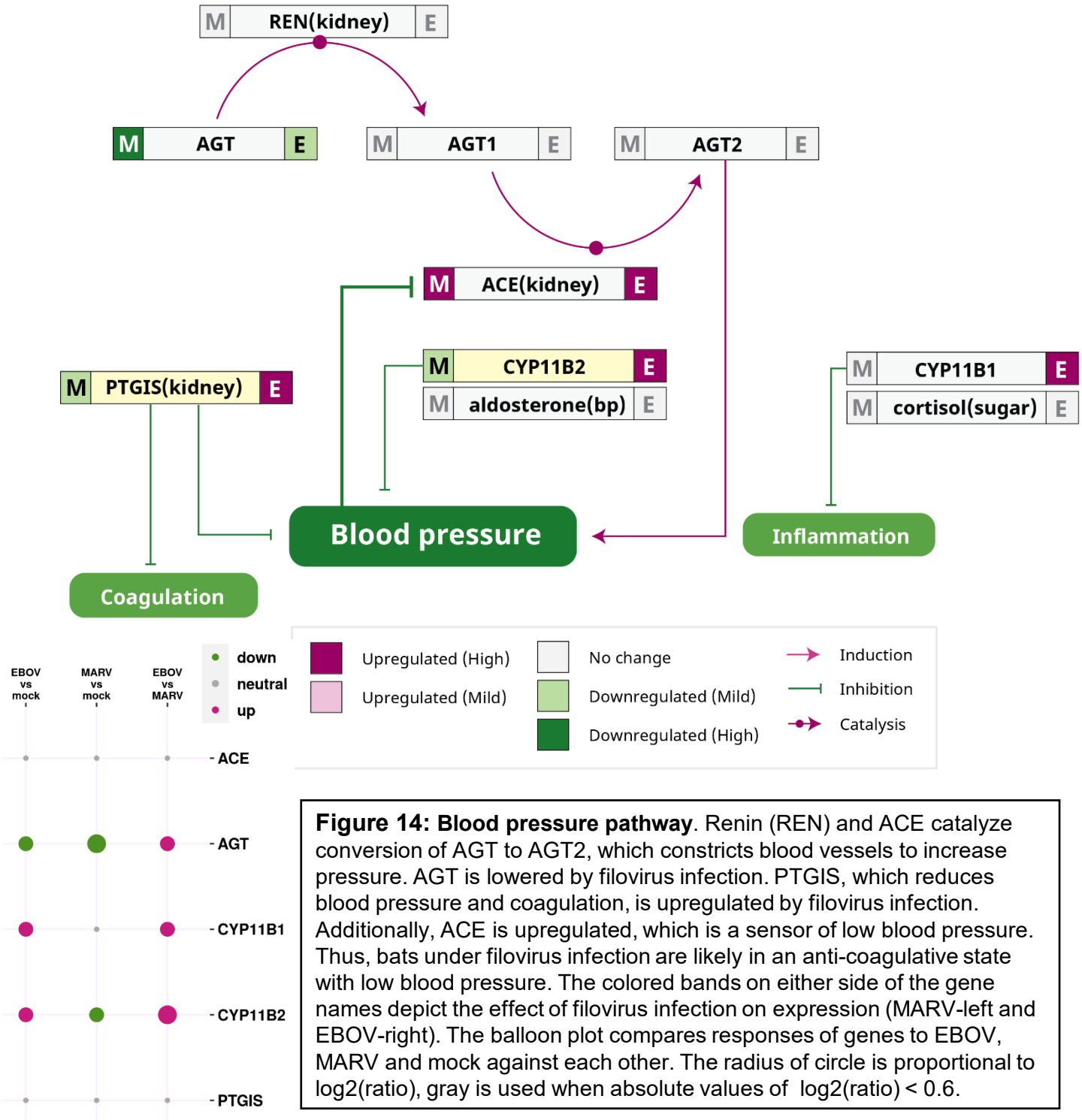

Figure 14: Blood pressure pathway. Renin (REN) and ACE catalyze conversion of AGT to AGT2, which constricts blood vessels to increase pressure. AGT is lowered by filovirus infection. PTGIS, which reduces blood pressure and coagulation, is upregulated by filovirus infection. Additionally, ACE is upregulated, which is a sensor of low blood pressure. Thus, bats under filovirus infection are likely in an anti-coagulative state with low blood pressure. The colored bands on either side of the gene names depict the effect of filovirus infection on expression (MARV-left and EBOV-right). The balloon plot compares responses of genes to EBOV, MARV and mock against each other. The radius of circle is proportional to log2(ratio), gray is used when absolute values of log2(ratio) < 0.6.

bioRxiv preprint doi: https://doi.org/10.1101/2020.04.13.039503; this version posted April 15, 2020. The copyright holder for this preprint (which was not certified by peer review) is the author/funder, who has granted bioRxiv a license to display the preprint in perpetuity. It is made available under aCC-BY 4.0 International license.

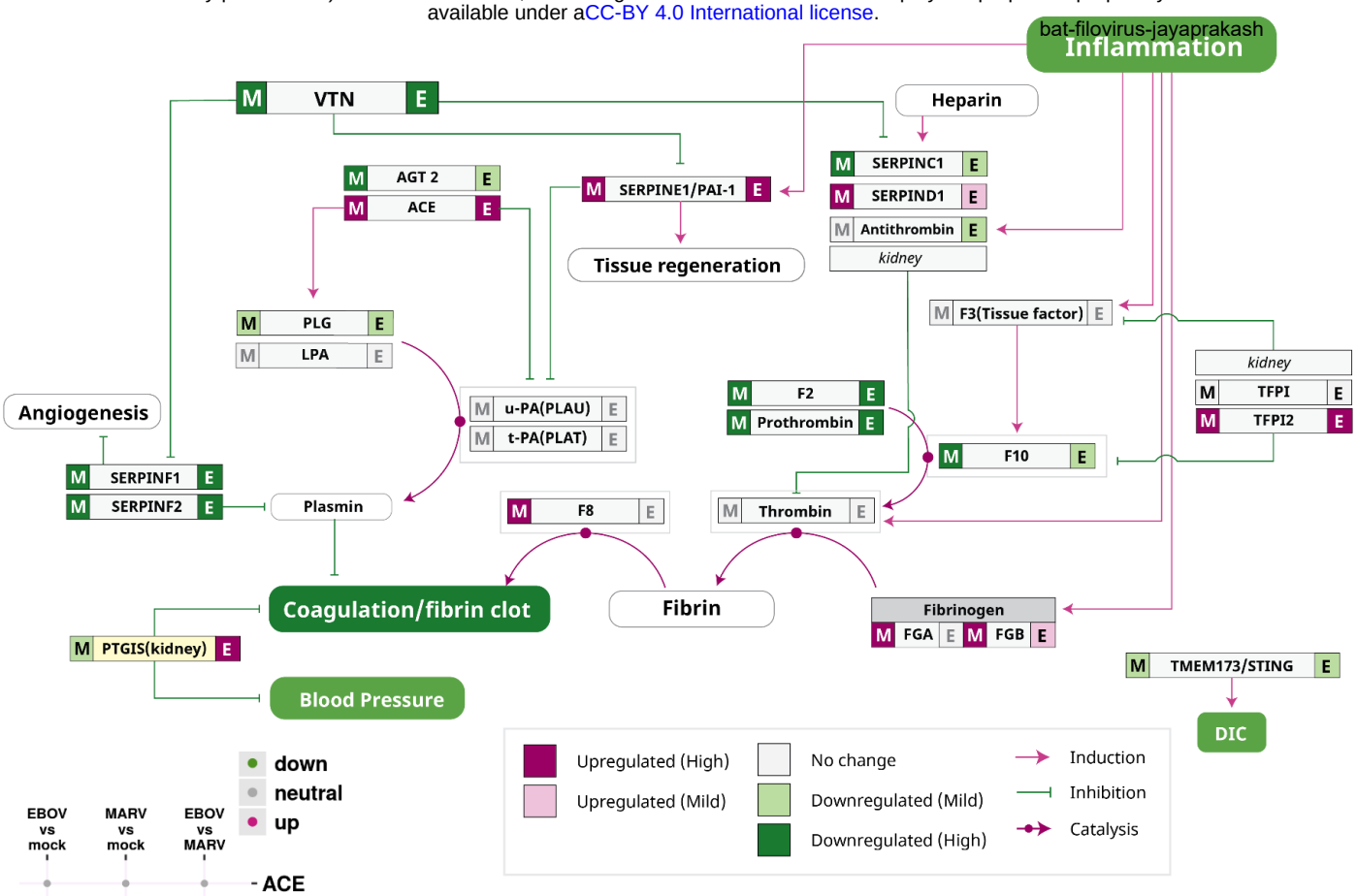

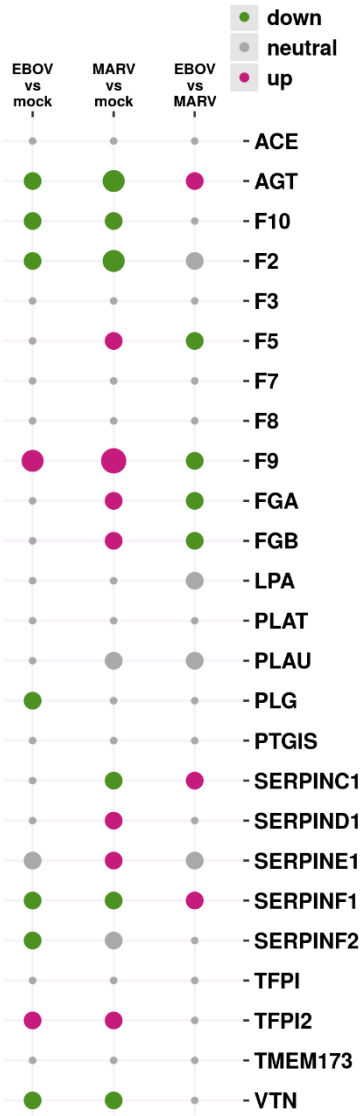

Figure 15: The coagulation pathway is a complex cascade of multiple factors, eventually leading to the formation of a clot. Except for F3, the tissue factor, all other proteases in the cascade require activation. Genes whose activation cannot be measured by mRNAseq are shown in white. Catalytic activity is represented by a red dot. The serine protease plasmin opposes this process by attacking the fibrin mesh to dissolve clots. Urokinase-type plasminogen activator (uPA, PLAU gene) activates plasminogen to generate plasmin. SERPINE1 (PAI-1) inhibits the activity of uPA, blocking the creation of Plasmin, thereby stabilizing clots. SERPINF2 also stabilizes clots by directly inhibiting plasmin. PTGIS creates prostacyclin, which prevents platelet aggregation, yet another path for inhibiting clot formation and coagulation. Prostacyclin is also a potent vasodilator. Failure in the control of plasmin (e.g. inactivation of SERPINF2 which inhibits plasmin) can lead to hemorrhagic diathesis, while blocking plasmin activity can lead to excessive clotting. Filovirus infection in bats leads to low F2 (which lowers fibrin) and raises levels of PTGIS which suggest that they are in a low coagulation state. The colored bands on either side of the gene names depict the effect of filovirus infection on expression (MARV-left and EBOV-right). The balloon plot compares responses of genes to EBOV, MARV and mock against each other. The radius of circle is proportional to log2(ratio), gray is used when absolute values of log2(ratio) < 0.6.

bioRxiv preprint doi: https://doi.org/10.1101/2020.04.13.039503; this version posted April 15, 2020. The copyright holder for this preprint (which was not certified by peer review) is the author/funder, who has granted bioRxiv a license to display the preprint in perpetuity. It is made available under aCC-BY 4.0 International license.

Tables

bioRxiv preprint doi: https://doi.org/10.1101/2020.04.13.039503; this version posted April 15, 2020. The copyright holder for this preprint (which was not certified by peer review) is the author/funder, who has granted bioRxiv a license to display the preprint in perpetuity. It is made available under aCC-BY 4.0 International license.

Positive APPs	MARV	EBOV
Serum Amyloid A (SAA1,SAA2)	UP	UP
Ceruloplasmin (CP)	UP	UP
Orosomucoid 2 (ORM2) Alpha1-Acid glycoprotein	UP	UP
Microsomal Glutathione S-Transferase (MGST1,MGST2)	UP	UP
Fibrinogen (FGA,FGB,FGG)	up	neutral
C4B	up	neutral
C3P1	up	neutral
Haptoglobin (HP)	neutral	neutral
Alpha2-Macroglobulin (A2M)		
C-reactive protein (CRP)	N/A	N/A
Negative APPs		
Albumin (ALB)	down	neutral
Transferrin (TF)	neutral	neutral
Transthyretin (TTR)	down	Down
Retinol Binding protein (RBP4)	neutral	Neutral

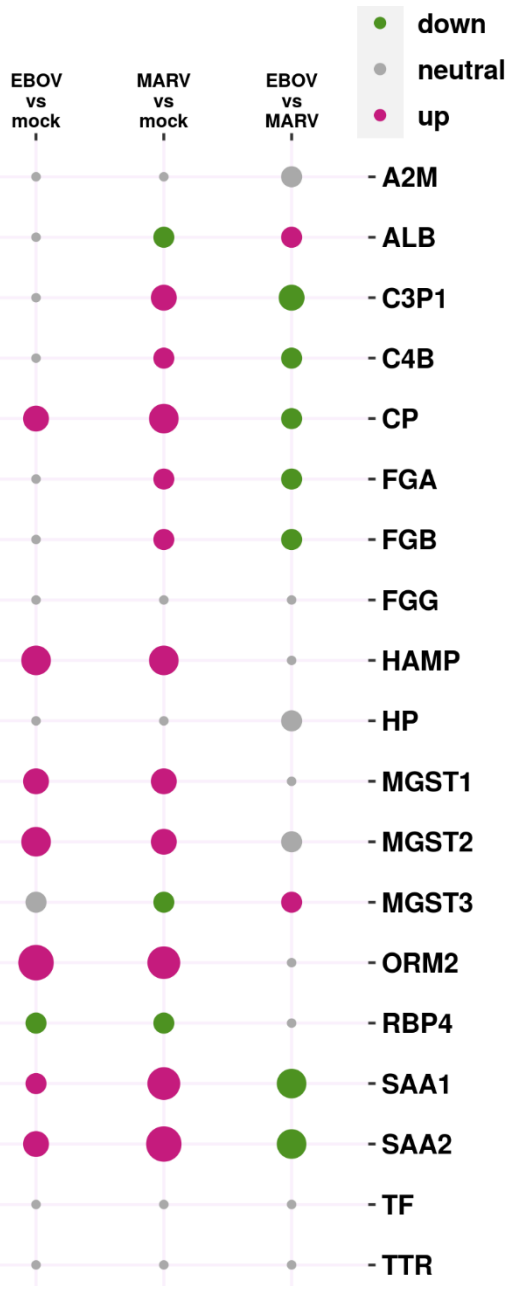

Table 1 Acute Phase Proteins respond strongly to inflammatory cytokines (IL-6, TNFα etc.). SAA1/2 is highly up regulated by the filovirus (MARV more than EBOV), as is ORM2 . CP, involved in copper/iron metabolism is also massively up regulated by MARV infection, while exhibiting a smaller effect in EBOV. CRP, used as a marker for acute phase response in humans, does not appear to be expressed in these bats.TF is highly expressed in all samples, but does not react to filoviral infection, while TTR is not expressed in any of the samples. "UP/up" stands for > 5/2-fold increase, "Neutral" is when expression did not change and "down" represents >2-fold decrease. The balloon plot compares responses of genes to EBOV, MARV and mock against each other. The radius of circle is proportional to log2(ratio), gray is used when absolute values of log2(ratio) < 0.6.

bioRxiv preprint doi: https://doi.org/10.1101/2020.04.13.039503; this version posted April 15, 2020. The copyright holder for this preprint (which was not certified by peer review) is the author/funder, who has granted bioRxiv a license to display the preprint in perpetuity. It is made available under aCC-BY 4.0 International license.

Supplementary Figures and Tables

bioRxiv preprint doi: https://doi.org/10.1101/2020.04.13.039503; this version posted April 15, 2020. The copyright holder for this preprint (which was not certified by peer review) is the author/funder, who has granted bioRxiv a license to display the preprint in perpetuity. It is made available under aCC-BY 4.0 International license.

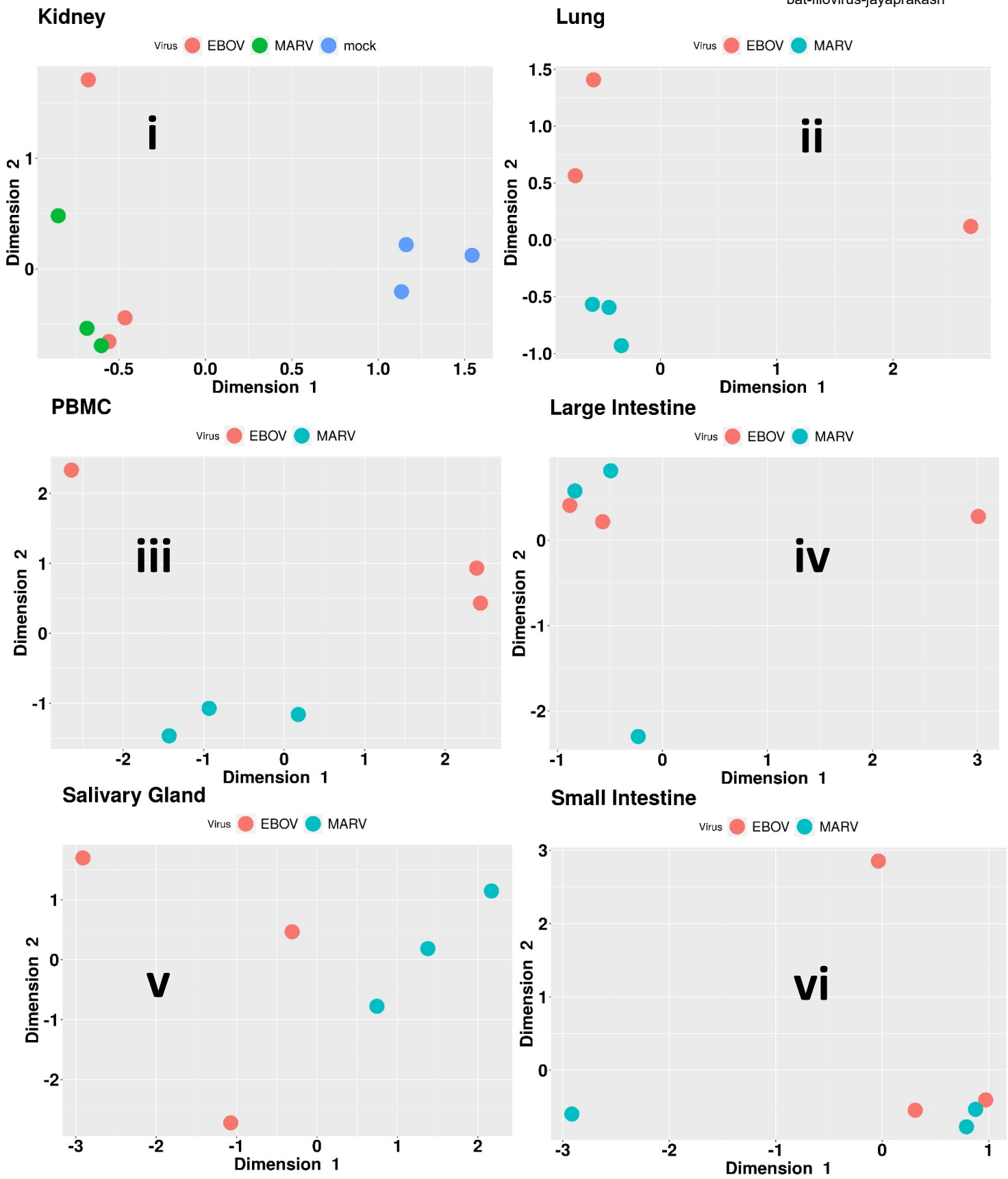

Figure S1. MDS plots along the two leading dimensions of top 500 genes by fold-change from non-infected(mock), EBOV-infected and MARV-infected samples from i) Kidney, ii) Lung, iii) PBMC, iv) Large intestine, v) Small intestine, vi) Salivary gland. Liver exhibits viral transcripts and shows the best separation (**Fig. 1**), but other organs show virus-specific signatures too, suggesting that there is a systemic response to the infection. We failed to recover good quality RNA from a few tissue samples, hence there are differences in the number of samples in individual plots.

bioRxiv preprint doi: https://doi.org/10.1101/2020.04.13.039503; this version posted April 15, 2020. The copyright holder for this preprint (which was not certified by peer review) is the author/funder, who has granted bioRxiv a license to display the preprint in perpetuity. It is made available under aCC-BY 4.0 International license.

Tissue	mock	EBOV	MARV
Liver	3	3	3
Lung	0	3	3
Spleen	3	3	3
Kidney	3	3	3
Salivary gland	0	3	3
Large intestine	0	3	3
Small intestine	0	3	3
Mesenchymal lymph node	0	3	0
Axial lymph node	0	3	0
Testes	0	0	1
PBMC	0	3	3

Table S1. List of bat samples. Bat tissues profiled using mRNAseq

bioRxiv preprint doi: https://doi.org/10.1101/2020.04.13.039503; this version posted April 15, 2020. The copyright holder for this preprint (which was not certified by peer review) is the author/funder, who has granted bioRxiv a license to display the preprint in perpetuity. It is made available under aCC-BY 4.0 International license.

Table S2 A Divergent genes upregulated by MARV and EBOV infection (I). Pathways involving vascular function, inflammation, mitochondria, lipid metabolism, tissue regeneration, Macrophages, T cell function and the complement are common themes running through these lists The balloon plot compares responses of genes to EBOV, MARV and mock against each other. The radius of circle is proportional to log2(ratio), gray is used when absolute values of log2(ratio) < 0.6.

gene	process
	vascular
HAMP /Hepcidin	cellular iron ion homeostasis inflammatory induces M1 macrophages
SRGN	platelet degranulation
AK3	platelet production nucleoside diphosphate phosphorylation mitochondrial
GLRX	antioxidant defense system VEGF expression vascular growth
CEBPZOS	blood cell maturation
	mitochondrial
MRPL50	organelle organization
GSTZ1	detox reduces oxidative stress
	redox
PECR	oxidation-reduction process lipid synthesis regeneration cellgrowth
GALM	glucose metabolic process
	Macrophages
APOL6	monocyte to macrophage differentiation lipid metabolism
TIMD4	expressed by macrophage maintains killer T cell activity
CCL18	attracts T cells to macrophages cellular response to IFNG
CXCL10	secreted by macrophage in response to IFNG role in hypertension immune response
CCL3	macrophage inflammatory protein cellular response to IFNG
PRXL2A	inhibits production of inflammatory cytokines by macrophages
S100A12	paralog of S100A8 IL-10 induced monocytes macrophages proinflammatory mast cell chemoattractant innate immune response
PLAC8	expressed by macrophage phospholipid metabolic process
ISG15	regulation of IFNG production Mito function in macrophages
CCL7	regulates macrophages attracts monocytes eosinophils but not neutrophils cellular response to interferon-gamma
	innate immunity
CLEC4F	endocytosis pathogen detector
CLECL1	expressed by dendritic and B cells enhances IL-4 production regulates immune response
CXCL3	chemoattractant for neutrophils immune response

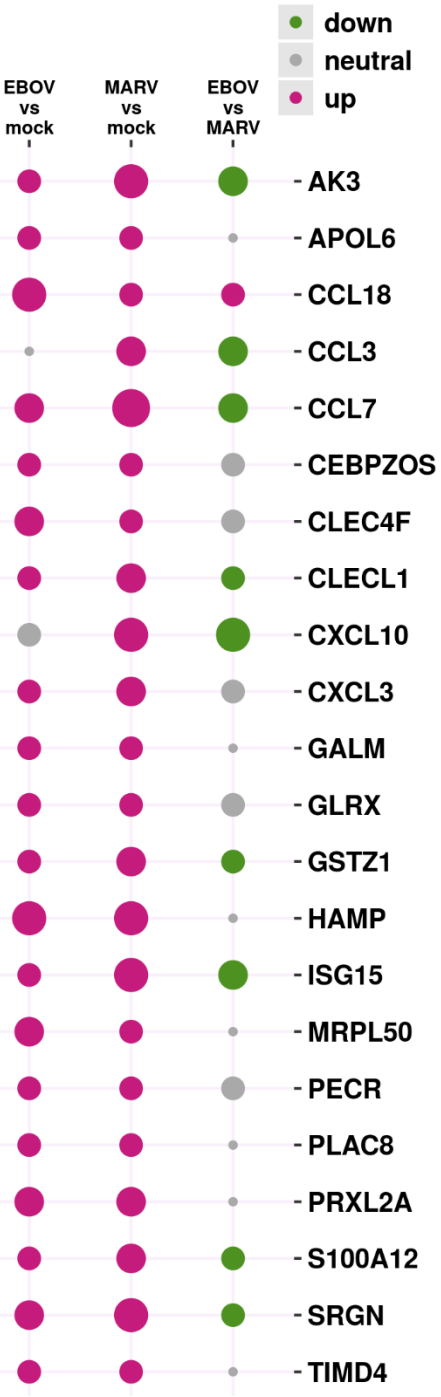

bioRxiv preprint doi: https://doi.org/10.1101/2020.04.13.039503; this version posted April 15, 2020. The copyright holder for this preprint (which was not certified by peer review) is the author/funder, who has granted bioRxiv a license to display the preprint in perpetuity. It is made available under aCC-BY 4.0 International license.

Table S2 B Divergent genes upregulated by MARV and EBOV infection (II). Pathways involving vascular function, inflammation, mitochondria, lipid metabolism, tissue regeneration, Macrophages, T cell function and the complement are common themes running through these lists The balloon plot compares responses of genes to EBOV, MARV and mock against each other. The radius of circle is proportional to log2(ratio), gray is used when absolute values of log2(ratio) < 0.6.

Gene	process
	T cell
LY6E	Tcell development negative regulator of monocytes dampens response
	Complement
MBL2	activates complement mannose-binding innate immune response
	Digestion
PRB1	digestion salivary proline-rich protein
	Toxins
UGT2A3	excretion of toxic compounds flavonoid biosynthetic process
	Inflammation
ORM2	acute phase reactant regulation of immune system process
IL1RN	IL-1R antagonist inhibits IL1A/B, modulates inflammation immune response
MGST2	generates LTC4 mediates stress
S100A8	leukocyte migration involved in inflammatory response
	tissue regeneration
ACOT13	essential for cell proliferation mitochondrial function (Macrophage M2)
S100P	cell proliferation, response to organic substance
NUDT16	positive regulation of cell proliferation
EIF4EBP3	negative regulation of translational initiation
	other
ZG16B	atherosclerosis retina homeostasis
SUB1	regulation of transcription from RNA polymerase II promoter
UNDEF108	
UNDEF771	

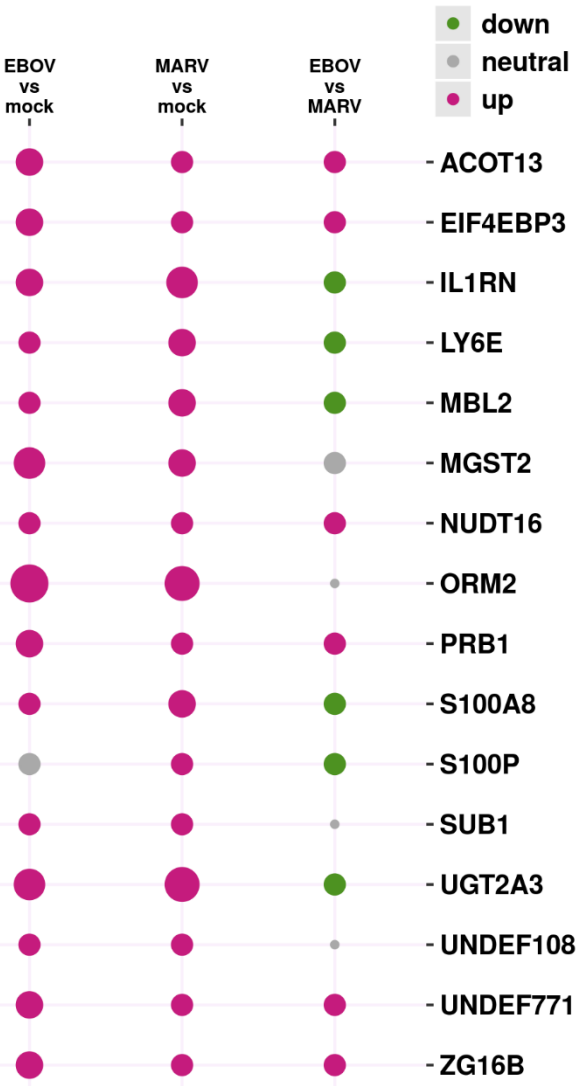

bioRxiv preprint doi: https://doi.org/10.1101/2020.04.13.039503; this version posted April 15, 2020. The copyright holder for this preprint (which was not certified by peer review) is the author/funder, who has granted bioRxiv a license to display the preprint in perpetuity. It is made available under aCC-BY 4.0 International license.

Table S3 A Divergent genes downregulated by MARV and EBOV infection (I). Pathways involving vascular function, inflammation, mitochondria, lipid metabolism, tissue regeneration, Macrophages, T cell function and the complement are common themes running through these lists. The balloon plot compares responses of genes to EBOV, MARV and mock against each other. The radius of circle is proportional to log2(ratio), gray is used when absolute values of log2(ratio) < 0.6.

gene	process
	mitochondria/oxidation/fatty-acid
MRPL54	organelle organization
CA3	Nitrogen metabolism bicarbonate transport
RNASEH1	mtDNA replication mutations lead to autoimmunity(T1D)
CHCHD7	protein import
CHCHD10	negative regulation of ATP citrate synthase activity
	vascular
ART4	Blood group antigens protein ADP-ribosylation
HRG	platelet degranulation Histidine-rich glycoprotein
MEG3	negative regulation of VEGF receptor signaling pathway
TMEM80	Increased transferrin (TF) endocytosis
	inflammation
AHSG	regulation of inflammatory response
CRELD2	ER-stress response
TEX264	stress , elevated platelet cytosolic Ca2+ responsive
	innate immunity
BTBD6	Class I MHC-mediated antigen processing/presentation
C8G	complement Complement component C8 gamma chain
EEF1D	positive regulation of I-kB kinase/NF-kB signaling
MIIP	down-regulates NFKB2 and ICAM1 inhibition of migration/invasion
TMEM80	Increased vaccinia virus (VACV) infection Decreased NF-kB reporter expression
CRIP1	cysteine-rich protein 1
	lipids
MOGAT1	triacylglycerol biosynthesis and Metabolism
	toxin
GSTA5	detoxification glutathione metabolic process
SLC17A2	Sodium/anion cotransporter family ossification
	macrophages
RNASET2	chemoattractants for macrophages and modulate the inflammatory processes
	vascular (iron)
ATP6V0D2	cellular iron ion homeostasis
BSG	carries OK antigens on red blood cells:cell surface receptor signaling pathway:inflammation
LCN2	sequesters iron (antibacterial) iron/toxin transport cisplatin resistance innate immune response

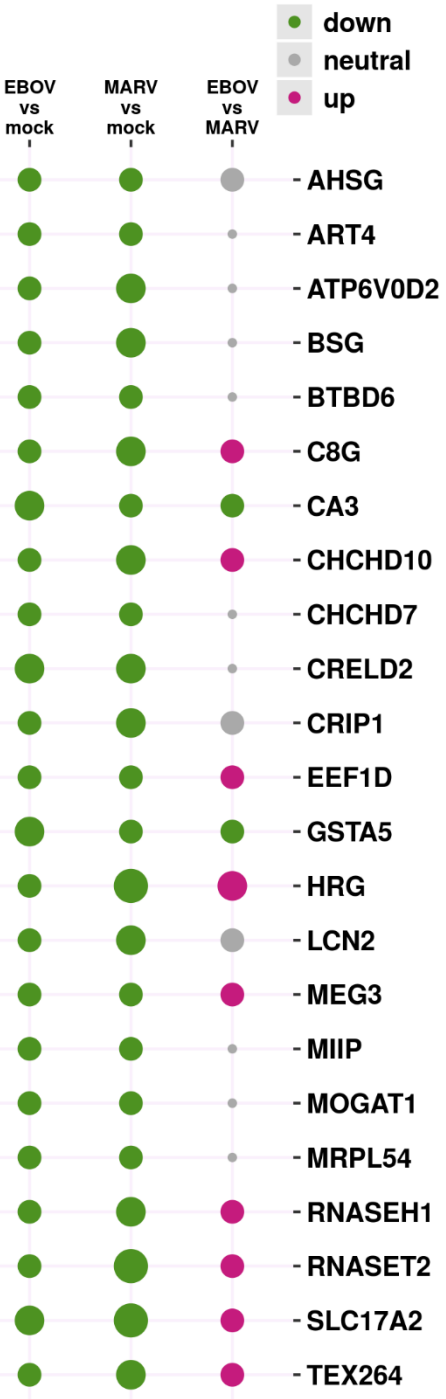

bioRxiv preprint doi: https://doi.org/10.1101/2020.04.13.039503; this version posted April 15, 2020. The copyright holder for this preprint (which was not certified by peer review) is the author/funder, who has granted bioRxiv a license to display the preprint in perpetuity. It is made available under aCC-BY 4.0 International license.

Table S3 B Divergent genes downregulated by MARV and EBOV infection (II). Pathways involving vascular function, inflammation, mitochondria, lipid metabolism, tissue regeneration, Macrophages, T cell function and the complement are common themes running through these lists The balloon plot compares responses of genes to EBOV, MARV and mock against each other. The radius of circle is proportional to log2(ratio), gray is used when absolute values of log2(ratio) < 0.6.

gene	process
	splicing
SNRPN	mRNA splicing via spliceosome
	T cell
GPX4	role in primary T-cell response to viral infection protects T-cells from ferroptosis supports T-cell expansion mitochondrial
	Metabolism
TSTD1	Thiosulfate sulfur transferase/rhodanese-like
NUDT14	Hydrolyzes UDP-glucose to glucose 1-phosphate and UMP and ADP-ribose to ribose 5-phosphate and AMP
	Digestion
FABP2	Fatty acid-binding protein intestinal
	Macrophages
APOC1	activated when monocytes differentiate to macrophages positive regulation of cholesterol esterification
	apoptosis/tissue regeneration
MSTO2P	Proliferation
LCMT1	regulation of apoptotic process
PRDM11	inhibits proliferation induces apoptosis
	Other
SPP2	negative regulation of endopeptidase activity
SCGB1C1	upper respiratory tract
RAMP1	regulation of GPCR signaling pathway
S100G	calcium ion/vitamin D binding mineral absorption
RANGRF	positive regulation of GTPase activity
RPS28	viral process
BEX4	
URAHP	
C19orf12	
FLJ37453	
TMEM141	
FXYD1	positive regulation of sodium ion export
UNDEF425	
UNDEF464	

bioRxiv preprint doi: https://doi.org/10.1101/2020.04.13.039503; this version posted April 15, 2020. The copyright holder for this preprint (which was not certified by peer review) is the author/funder, who has granted bioRxiv a license to display the preprint in perpetuity. It is made available under aCC-BY 4.0 International license.

Table S4 Divergent genes upregulated by MARV infection. Pathways involving vascular function, inflammation, mitochondria, lipid metabolism, tissue regeneration, Macrophages, T cell function and the complement are common themes running through these lists. The balloon plot compares responses of genes to EBOV, MARV and mock against each other. The radius of circle is proportional to log2(ratio), gray is used when absolute values of log2(ratio) < 0.6.

gene	process
	macrophages
BPI	negative regulation of IL-6 production expressed by macrophages Bactericidal permeability-increasing protein
	Complement
CD46	inactivates C3b and C4b protect host cell from damage by complement innate immune response
	apoptosis
XAF1	response to interferon-beta proapoptotic
TNFRSF10A	activation of NF-kB-inducing kinase activity cell apoptosis
BID	positive regulation of apoptotic process
	mitochondria/glycolysis/fatty-acid
SPR	oxidoreductase activity and aldo-keto reductase (NADP) activity nitric oxide biosynthetic process
ECHDC3	fattyacidpathways(Macrophage M2)
	innate immunity
IFI30	antigen processing IFNG-mediated signaling pathway
TRIM22	IFNG-mediated signaling pathway antiviral ubiquitinates viral proteins
ICAM1	IFNG-mediated signaling pathway
	inflammation
IL33	positive regulation of inflammatory response
	digestion
SULT2A1	digestion Bile salt sulfotransferase
	T cells
CMTM6	protects PD-L1 inhibits T cells
GZMH	immune response T cell Granzyme H
	Vascular
EMP2	positively regulates VEGF-A , integrin-mediated signaling pathway
RHOG	platelet activation Rho-related
	other
ARF1	viral process ADP-ribosylation factor 1
RBM12B-AS1	RBM12B antisense RNA 1
RNF213	protein ubiquitination E3 ubiquitin-protein ligase RNF213
UNDEF25	
CUNH17of100	
UNDEF113	
marburg	Marburg virus

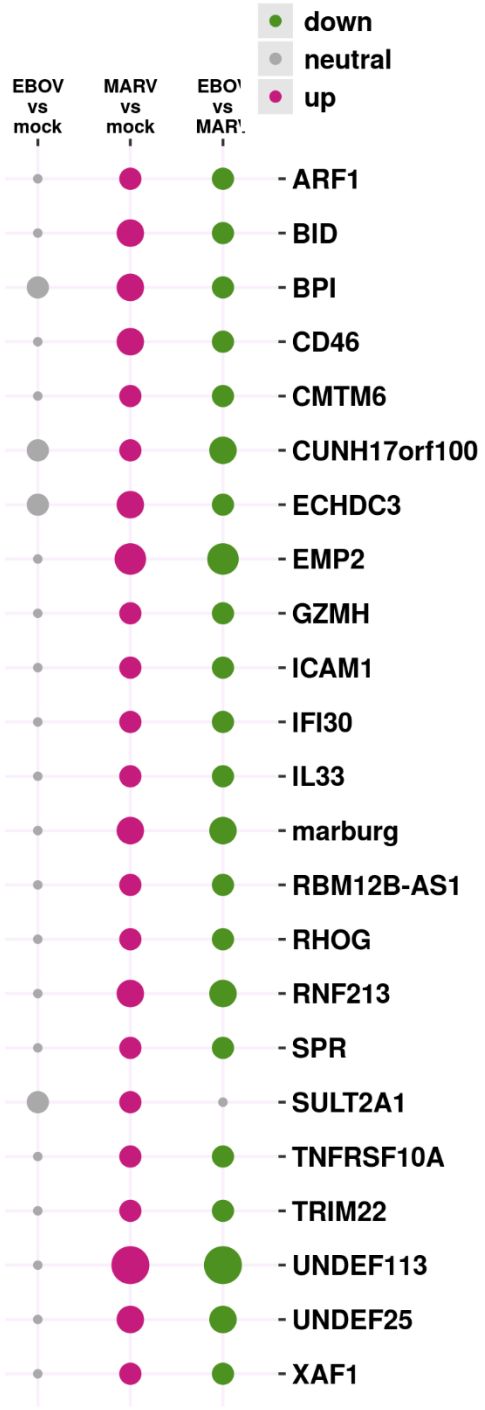

bioRxiv preprint doi: https://doi.org/10.1101/2020.04.13.039503; this version posted April 15, 2020. The copyright holder for this preprint (which was not certified by peer review) is the author/funder, who has granted bioRxiv a license to display the preprint in perpetuity. It is made available under aCC-BY 4.0 International license.

Table S5 Divergent genes downregulated by MARV infection. Pathways involving vascular function, inflammation, mitochondria, lipid metabolism, tissue regeneration, Macrophages, T cell function and the complement are common themes running through these lists. The balloon plot compares responses of genes to EBOV, MARV and mock against each other. The radius of circle is proportional to log2(ratio), gray is used when absolute values of log2(ratio) < 0.6.

gene	process
	Mitochondrial
MRPL41	translation
NDUFV3	mitochondrial electron transport NADH to ubiquinone
MDH2	gluconeogenesis mitochondrial
TOMM6	protein targeting to mitochondrion
NDUFB11	respiratory electron transport chain
ATP5MPL	mitochondrial membrane atp synthase
NDUFB1	mitochondrial electron transport NADH to ubiquinone
NDUFA4	mitochondrial electron transport NADH to ubiquinone
COA3	positive regulation of mitochondrial translation
UQCRBP1	ubiquinol-cytochrome c reductase binding protein pseudogene 1
	inflammation/oxidative stress
NDUFB4	response to oxidative stress
	Digestion
AMY2B	digestion Alpha-amylase 2B
	Vascular
SERPINA4	negative regulation of endopeptidase activity
ZNF24	represses VEGF vascularization myelination
	innate immune(complement)
C4BPB	innate immune response
CCL16	cellular response to interferon-gamma
RPS27A	toll-like receptor signaling pathway
	apoptosis/tissue regeneration
ATF4	positive regulation of apoptotic process
JTB	Inhibits apoptosis induced by TGFB1
SIVA1	viral entry into host cell apoptosis regulation
	Splicing
RBM8A	regulation of alternative mRNA splicing via spliceosome
	other
RPL4	viral process
RPL18A	viral process
RPL22	viral process
RPLP1	viral process
RPS17	viral process
RPSAP58	ribosomal small subunit assembly
RPP25L	Ribonuclease P protein subunit p25-like protein
CUNH6orf226	

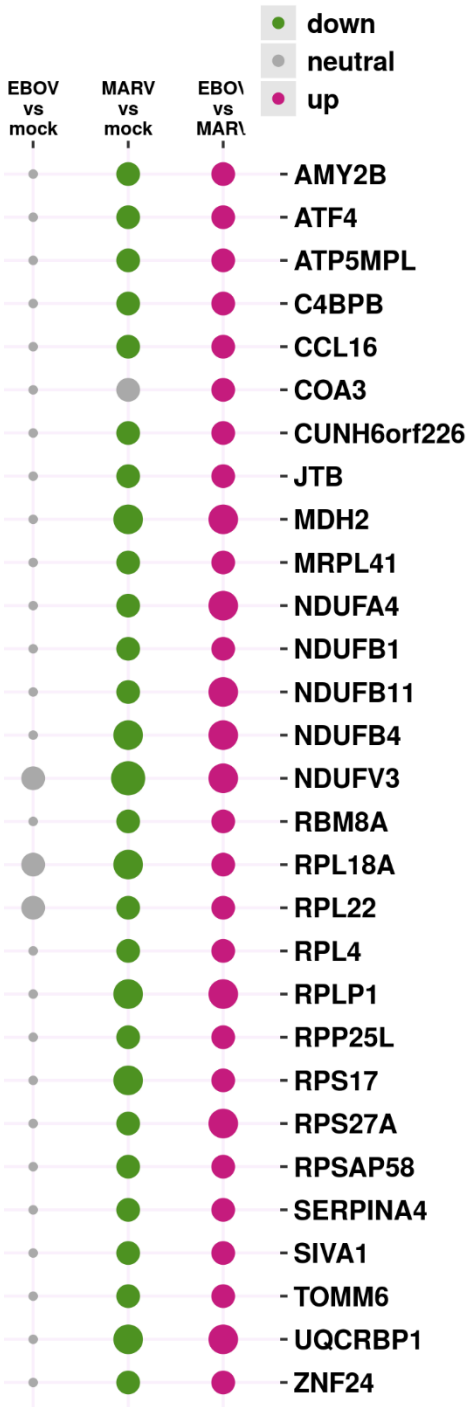

bioRxiv preprint doi: https://doi.org/10.1101/2020.04.13.039503; this version posted April 15, 2020. The copyright holder for this preprint (which was not certified by peer review) is the author/funder, who has granted bioRxiv a license to display the preprint in perpetuity. It is made available under aCC-BY 4.0 International license.

Table S6 Divergent genes upregulated by EBOV infection. Pathways involving vascular function, inflammation, mitochondria, lipid metabolism, tissue regeneration, T cell function and the complement are common themes running through these lists. The balloon plot compares responses of genes to EBOV, MARV and mock against each other. The radius of circle is proportional to log2(ratio), gray is used when absolute values of log2(ratio) < 0.6.

gene	process
	vascular
CYP11B2	regulation of blood volume by renal aldosterone Cytochrome P450 11B2 mitochondrial
TMEM133/ARHGAP42	inhibits RhoA activity to regulate vascular tone and control blood pressure
	inflammation/stress
CYP11B1	cortisol production stress response immune response Cytochrome P450 11B1 mitochondrial
	mitochondrial
MRPS33	translation 28S ribosomal protein S33
PET100	respiratory chain complex IV
NDUFA5	respiration electron transport NADH to ubiquinone
	lipid/fatty-acid
ADIRF	lipid metabolism
	tissue regeneration
H19	lincRNA cell growth control
CENPW	mitotic cell cycle
	Other
LINC00467	lincRNA 467
UNDEF312	

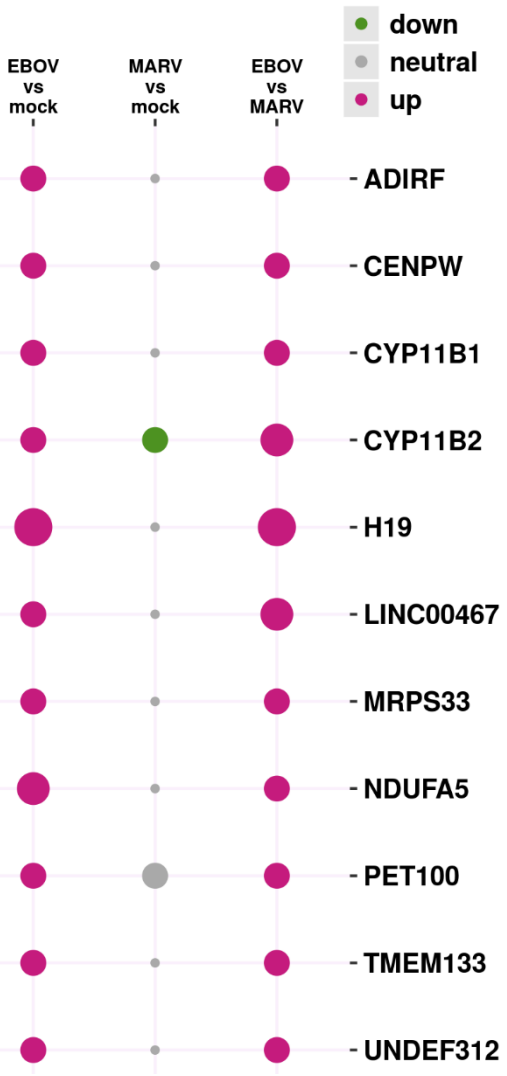

bioRxiv preprint doi: https://doi.org/10.1101/2020.04.13.039503; this version posted April 15, 2020. The copyright holder for this preprint (which was not certified by peer review) is the author/funder, who has granted bioRxiv a license to display the preprint in perpetuity. It is made available under aCC-BY 4.0 International license.

Table S7 Divergent genes downregulated by EBOV infection. Only 3 known genes, from innate immunity, vascular(coagulation) and Digestion, which seems to occur occasionally in these list of genes (probably related to liver function) . The balloon plot compares responses of genes to EBOV, MARV and mock against each other. The radius of circle is proportional to log2(ratio), gray is used when absolute values of log2(ratio) < 0.6.
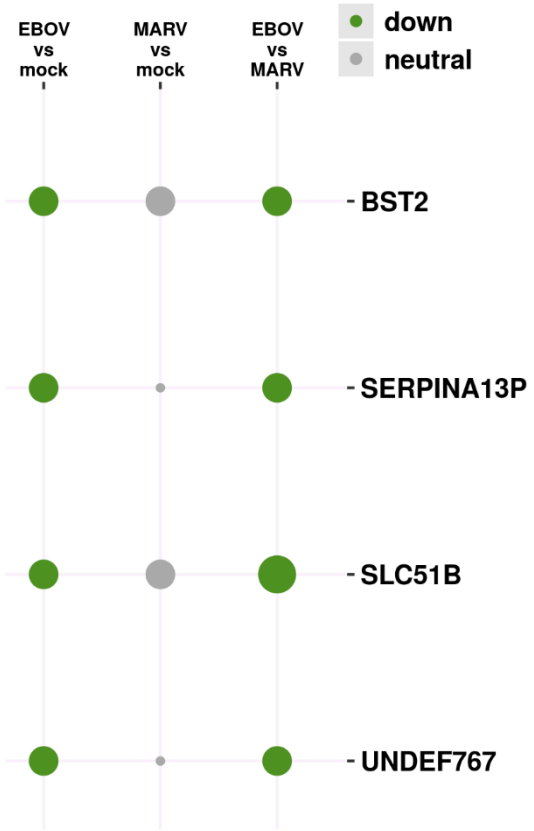
gene	process
	innate immunity
BST2	response to IFNG
	vascular
SERPINA13P	protease inhibitor clotting
	digestion
SLC51B	bile secretion
	other
UNDEF767